

**Development and Demonstration of Nano-sized TiO₂ –
based Photocatalytic Oxidation Technology for
Controlling VOCs**

(Final Report)

Submitted to
**Ministry of Environment, Forests and Climate Change
(MoEFCC)**



**Mukesh Sharma; PhD
Centre for Environmental Science and Engineering
Indian Institute of Technology Kanpur**

October 2016

Acknowledgements

The project, “Development and Demonstration of Nano-sized TiO₂-based Photocatalytic Oxidation Technology for Controlling VOCs” was sponsored by the Ministry of Environment, Forests and Climate Change (MoEFCC) to the Indian Institute of Technology, Kanpur. The project was quite vast in terms of activities including field sampling, data collection, laboratory analyses, computational work, interpretation of results and pilot testing of the developed technology/equipment. Although it will be an endeavor to remember and acknowledge all those who assisted in the project, we seek pardon in anticipation, if we err.

We gratefully acknowledge the support and guidance received from Dr. Rajneesh Dubey, former Joint Secretary, MoEFCC, Dr. Rashid Hasan, Sr. Advisor, Dr. H. Kharkwal and Dr. M. Salahuddin Scientists, MoEFCC. The suggestions of expert members of Project Management Committee, Prof. A.K. Nema, IIT Delhi, Prof K.C. Gupta, IITR, Lucknow, Prof. A.B. Gupta, MNIT Jaipur, and Prof. Mohammad Rafat are gratefully acknowledged.

Support of Aarti Industries Ltd. Vapi and other institutions is gratefully acknowledged. Shri Kirit Mehata, Director, Aarti Industries, Vapi, Shri N.C. Patel, Clean Enviro Projects Consultancy Pvt Ltd, Vapi and Dr. Rajendra Prasad, Ecotech, Greater Noida were instrumental in project implementation and assisted in all field sampling and provided technical advice; we gratefully acknowledge their support.

Mr. Indramani Dhada, Mr. Pavan Kumar Nagar, PhD Scholars and Mr. Dharendra Singh, Senior Project Engineer, IIT Kanpur worked tirelessly from field sampling to analysis and preparation of report; thanks to Indramani, Pavan and Dharendra for their inestimable support.

Table of Content

Acknowledgements	i
Table of Content	ii
List of Tables	iv
List of Figures	v
Executive Summary	vii
1 Introduction	1
1.1 Background	1
1.2 PCO Technology	4
1.3 Factors Influencing PCO	4
1.3.1 Choice of Catalyst	5
1.3.2 Characteristics of TiO ₂ Coating	6
1.3.3 Temperature	7
1.3.4 Relative Humidity	7
1.3.5 Concentration of Pollutants	8
1.3.6 Ultra Violet Irradiation	9
1.3.7 Photocatalyst Deactivation	9
1.3.8 Brunauer, Emmett and Teller (BET) Surface Area	10
1.4 Degradation Rate Constant and Regeneration	10
1.5 Intermediates and Associated Risk	11
2 Materials and Methods	14
2.1 Improving PCO Technology	14
2.2 Field Application of Technology	20
2.3 Risk Characterization of Exposure to Intermediates	24
3 Improving PCO Technology: Designing, Coating and Regenerating Catalyst	27
3.1 Characterization of Coatings	27
3.2 Kinetic of VOCs Degradation in Batch Reactor	31
3.3 Regeneration of Catalyst	35
3.4 Discussion	37
4 Field Application: Results and Discussion	40
4.1 Case-1: Laboratory Using Benzene as Solvent	40
4.2 Case-2: Conference Room of A Solvent Industry Using MCB, DCB and TCB	41

4.3 Case-3: laboratory Using Multiple VOCs (Dichloromethane, Methanol, Ethyl acetate, Acetone, Hexane)	47
4.4 Pilot Testing	48
4.4.1 Second Pilot Testing (July 17-22, 2014)	48
4.4.2 Performance of VOC Control System	50
4.4.3 Interpretation of Results of pilot Testing and Way forward	61
4.5 The New Control Equipment	62
5 Risk Characterization of Exposure to Intermediates	66
5.1 Solid Phase Intermediates of Benzene	66
5.2 Intermediates of EXT	68
5.2.1 Vapour Phase	68
5.2.2 Solid Phase	70
5.3 Risk Assessment of Intermediates	73
5.3.1 Risk Assessment of Exposure to Intermediates of Benzene	73
5.3.2 Risk assessment of Exposure to Intermediates of EXT	74
6 Summary and Conclusions	78
6.1 Summary	78
6.2 Conclusions	79
References	82
Appendix- A	91
Appendix-B	92

List of Tables

Table 2.1: Adhesion tests	17
Table 2.2: Inlet VOC concentrations considered for this study	18
Table 2.3: Description of case studies, concentration of VOCs and physical parameters	21
Table 2.4: VOCs studied for intermediates	24
Table 3.1: Composition of different elements in TiO ₂ coated thin film	29
Table 3.2: Degradation rate Constants (k) for VOCs in min ⁻¹ m ⁻² of TiO ₂ surface area (estimated from first two hour of operation of reactor)	33
Table 3.3: Degradation rate constants (k) of VOCs in min ⁻¹ m ⁻² of TiO ₂ surface area over time	34
Table 4.1: VOC Emission and Control at Site-1	50
Table 4.2: VOC Emission and Control at Site-2 (Pump in operation)	51
Table 4.3: VOC Emission and Control at Site-3	53
Table 4.4: VOC Emission and Control at Site-3	53
Table 4.5: VOC Emission and Control at Site-4 on 18/07/2014 and 19/07/2014	56
Table 4.6: VOC Emission and Control at Site-5	59
Table 5.1: Mass of intermediates produced from PCO of ethylbenzene	69
Table 5.2: Mass of intermediates produced from PCO of xylenes and toluene (Vapour phase)	70
Table 5.3: Mass of intermediates released from PCO of EXT (µg per mg of EXT removed per sq-meter surface area of catalyst coating in 12hour continuous operation; solid phase)	73
Table 5.4: Indoor air concentration of intermediates (solid phase) and health risk (Volume of room 195 m ³ and mass of benzene treated 1.108 mg in 12 hours of operation)	74
Table 5.5: Indoor air concentration of intermediates (vapour and solid phase) of PCO of ethylbenzene and health risk (Volume of room 195 m ³ and mass of ethylbenzene treated 1.188 mg)	75

List of Figures

Figure 1.1: summary of major tasks and adopted approach	13
Figure 2.1: TiO ₂ coated reactors with teflon caps	15
Figure 2.2: Schematic of experimental set up for continuous operation of photoreactor	17
Figure 2.3: Full-scale VOC control device (schematic)	21
Figure 2.4: TiO ₂ coated chips for analysis	22
Figure 3.1: FE-SEM image showing the surface morphology for TiO ₂ nanoparticles (a) at 10 μ m (b) at 100 nm resolution (Dhada et al., 2015 b)	28
Figure 3.2: XRD pattern: 2 θ v/s intensity graph	28
Figure 3.3: EDAX spectra of TiO ₂ coated thin film	29
Figure 3.4: AFM image of TiO ₂ coated thin film (Dhada et al., 2015 b)	30
Figure 3.5: UV spectra of coating and band gap; (a) absorbance spectra, (b) transmittance spectra and (c) determination of the band gap for TiO ₂ coated glass substrate (Dhada et al., 2015 b)	31
Figure 3.6: PCO of various VOCs: BTEX in batch reactor in presence of 8W UV lamp	33
Figure 3.7: Variation in degradation kinetics over time for PCO of benzene in presence of 8W UV lamp (Dhada et al., 2015 b)	34
Figure 3.8: Catalyst regeneration methods (for PCO of benzene) (Dhada et al., 2015 b)	36
Figure 3.9: FE-SEM image showing the surface morphology for TiO ₂ nanoparticles at 10 μ m after 100 times of regeneration	37
Figure 4.1: Performance of control device for degradation of benzene	41
Figure 4.2: Schematic of conference room and installed VOC control system	42
Figure 4.3: Modelled and observed TVOC concentrations at the device	45
Figure 4.4: Ratio of steady state TVOC concentration inside the room and entering the room versus number of devices for Case-2	46
Figure 4.5: Performance of control device for degradation of TVOC in chemistry laboratory	48
Figure 4.6: Testing the VOC control device	49
Figure 4.7: VOC Emission and Control at Site-1	51
Figure 4.8: VOC Emission and Control at Site-2	52

Figure 4.9: VOC Emission and Control at Site-3	53
Figure 4.10: Long-term VOC Emission and Control at Site-3	55
Figure 4.11: VOC Emission and Control at Site-4 on 18 th and 19 th July 2014	58
Figure 4.12: Testing of mini-pilot plant at site-5	58
Figure 4.13: VOC Emission and Control at Site-5	60
Figure 4.14: Images of the New VOC Control System	65
Figure 5.1: Mass of intermediates (μg) adsorbed on the catalyst for each mg of benzene removed per sq-metre surface area of catalyst coating (8 hour operation)	67
Figure 5.2: Mass of intermediates (μg) adsorbed on the catalyst for each mg of ethylbenzene removed per sq-meter surface area of catalyst coating	71
Figure 5.3: Mass of intermediates (μg) adsorbed on the catalyst for each mg of p,m-xylene removed per sq-meter surface area of catalyst coating	71
Figure 5.4: Mass of intermediates (μg) adsorbed on the catalyst for each mg of o-xylene removed per sq-meter surface area of catalyst coating	72
Figure 5.5: Mass of intermediates (μg) adsorbed on the catalyst for each mg of toluene removed per sq-meter surface area of catalyst coating	72
Figure 5.6: Carcinogenic risk for vapour and solid phase (except benzene) intermediates of BTEX	76
Figure 5.7: Hazard index for vapour and solid phase (except benzene) intermediates of BTEX	76

Executive Summary

Volatile organic compounds (VOCs) of anthropogenic origin are important air pollutants emitted largely by industries, vehicles and domestic cooking using fossil fuels, especially bio-fuels. Many VOCs (e.g., benzene, toluene, ethylbenzene and xylene (BTEX)) are toxic and some are carcinogenic, mutagenic or teratogenic. The recent research efforts for removal of VOCs have focused on advanced oxidation processes such as photo catalytic oxidation (PCO) in presence of semiconductor photocatalyst. In PCO, formation of hydroxyl radical in presence of water vapour is primarily responsible for converting organic compounds into simple products such as water vapour and carbon dioxide. The titanium-di-oxide (TiO_2) based PCO of VOCs has high potential for cleaning industrial emissions and indoor air. However, the field application of PCO related technology for VOC control remains a challenge due to many issues that need to be addressed. The challenges include particle size of TiO_2 , effective coating, activation and deactivation of catalyst surface, uncertainties in estimated degradation rate constant and long-term application of PCO technology. Further, the complete oxidation of VOCs does not happen instantly. Some intermediates will be formed due to partial oxidation and may be harmful to the building occupants.

To address the above issues, this project has focused on: (i) laboratory study for improving PCO technology (ii) field applications of technology and (iii) characterizing the risk of exposure to intermediates and suggesting degradation pathways of BTEX. Based on the analyses and interpretations of results, insights acquired in the PCO processes can lead the technology for wider acceptance and field applications.

Based on characterization of catalyst surface for structural continuity, surface roughness, surface impurities, strong surface attachment and particle size, a standardized sol

gel coating method was established to apply TiO_2 on borosilicate glass substrate. The particle size of coated TiO_2 was in nano size (10.2 ± 1.43 nm) that should ensure large active surface area (around $100 \text{ m}^2/\text{g}$) of catalyst. This study has estimated the degradation rate of BTEX for ultra violet (UV) lamps of 8W, 11W and 16W. The highest degradation rate (for all VOCs) was obtained for 16WUV lamp. The high wattage of lamp results in increased running cost but there is an opportunity to optimize the process based on increased wattage versus increased efficiency of the PCO system.

For a stable performance of the reactor, the challenge was to accommodate continuous deactivation of the catalyst surface which adversely affects the degradation rate constant, k . For a thirteen hour operation and catalyst regeneration cycle, the average value of k (for BTEX) ranged from $0.80 \text{ min}^{-1} \text{ m}^{-2}$ to $0.95 \text{ min}^{-1} \text{ m}^{-2}$ for 8W UV lamp and $1.00 \text{ min}^{-1} \text{ m}^{-2}$ to $1.66 \text{ min}^{-1} \text{ m}^{-2}$ for 16W UV lamp. It was proposed that for 8W UV lamps, the k value should be taken as $0.87 \text{ min}^{-1} \text{ m}^{-2}$ (average of the range of k value) and for 16W UV lamps, it should be $1.3 \text{ min}^{-1} \text{ m}^{-2}$.

Three methods of catalyst regeneration (heating at 450°C , washing with H_2O_2 (strong oxidising agent) and irradiation by UV light) were examined to remove/oxidize deposited organic stick to the catalyst. Although these methods can regenerate the catalyst in the range 92-98 percent of original k value, heating of reactor was the fastest and most efficient regeneration technique and should be followed.

After addressing the impending challenges, the technology was taken to field after scaling up the laboratory reactor to pilot plant. The effectiveness of technology for different VOCs (benzene, chlorobenzenes (mono, di and tri) and mixture of solvents present in chemistry laboratory) was established. It was noted that the estimated degradation rate

constant for coexisting multiple VOCs was $1.06 \text{ min}^{-1} \text{ m}^{-2}$ (surface area of catalyst), which in comparison to that of benzene ($1.6 \text{ min}^{-1} \text{ m}^{-2}$), is smaller by 34 percent because of concurrent competitive reactions on the surface of catalyst. The control efficiency of device was over 99 percent for benzene, 88 percent for multiple VOCs and 71 percent for chlorobenzenes.

The intermediates of degradation of BTEX (both in vapour phase (except benzene) and those from catalyst regeneration) were quantified and human health risk of exposure of these intermediates was assessed. The carcinogenic risk and hazard index (HI) both were within acceptable level and technology can be adopted in field without any fear of unacceptable risk from the intermediates.

The major focus of the project was to pilot test the technology in the field and addresses all the issues of technology up-gradation. Specifically new equipment was designed based on the degradation rates estimated from laboratory studies (carried out in this project) reduction in the efficacy of catalyst with its use. The impediment and difficulties encountered in earlier versions have been taken in consideration while designing the new units which is easy to operate and cost effective as pressure drop has been reduced significantly. The technology is at a stage where it can be adopted by the industry.

1.1 Background

Volatile organic compounds (VOCs) are important air pollutants emitted largely by industries, vehicles and domestic cooking using fossil fuels, especially bio-fuels. Many VOCs (e.g. benzene, ethylbenzene and n-decane) are toxic and some are carcinogenic, mutagenic or teratogenic (Edgerton et al., 1989; Burstyn et al., 2007; You et al., 2008). Besides health effects, VOCs can combine with nitrogen oxides leading to production of secondary air pollutants (ozone, peroxy-acetyl nitrates and organic aerosols)(Carp et al., 2004; USEPA 2006; Song et al., 2007). Out of several VOCs, the common VOCs which are toxic and present in appreciable quantities in ambient air include benzene, toluene, ethylbenzene and xylene (BTEX) (Lau and Chan, 2003; Lü et al., 2006; Zhang et al., 2012). The major sources of BTEX are vehicular exhausts and evaporation losses from handling, distributing and storing of solvents (Srivastava et al., 2005; Choi et al., 2009; Dutta et al., 2009).

Increasing levels of VOCs in ambient air, indoor air and industrial premises (Mo et al., 2009a; Dhada et al., 2012) necessitate that VOC control technologies are developed and further improved. Earlier studies (Deshusses and Webster 2000; Rene et al., 2005), have reported that VOCs from polluted air streams can be controlled by traditional methods such as adsorption, condensation and incineration. Although these methods use simple techniques, there are certain implementation constraints which include high cost, unpredictable recoveries and difficulty in separating one or more VOCs for reuse/recycle (Jeong et al., 2005).

Advanced oxidation processes such as thermal oxidation and photo-catalytic oxidation (PCO) are promising technologies for control of VOCs (Carp et al., 2004; Everaert

and Baeyens, 2004). Thermal catalytic oxidation requires high temperatures of 200–1200°C for efficient operation. This is an expensive method and economically not feasible at low VOC concentrations (Wang et al., 2007). Ultraviolet (UV)-induced PCO techniques have been extensively studied and could be effective in controlling VOCs even at room temperature (Ao et al., 2003; Jeong et al., 2005).

In the PCO systems, accelerated oxidation of chemicals is achieved with the help of UV light and semiconductors as catalyst (Hager and Bauer, 1999). Usually, semiconductor materials enhance the photo catalytic reaction by lowering the required activation energy of the reaction due to their special electronic band structure (Puddu et al., 2010). The desirable properties of titanium dioxide (TiO₂) in terms of catalytic activity, chemical stability, non-toxicity, relatively inexpensive and availability make it a suitable photo catalyst (Hong, 2006).

The TiO₂ based PCO of VOCs has high potential for cleaning industrial emissions and indoor air (Mo et al., 2009a). However, the commercial application of PCO related technology for VOC control remains a challenge. It needs to be recognized that while the technology in theory and at laboratory scale is well established but there are many issues those need to be resolved and operational parameters optimized. The challenges include particle size of TiO₂, effective coating, activation and deactivation of catalyst surface, low photo-catalytic conversion of VOCs, uncertainties in estimated degradation rate constant (time⁻¹ per unit surface area), carbon balance (to estimate extent of mineralization of VOCs), catalyst deactivation/regeneration and designing and long-term operation of the reactor. Development of photo catalytic device for controlling VOCs in indoor air with proper model is needed to know the kinetics of degradation of VOC and extent of treatment required. The complete mineralization of VOCs does not happen instantly. Some intermediates will be

formed due to partial oxidation (Blount and Falconer, 2002) and can get released in the indoor air. These intermediates may be harmful to the building occupants, sometimes even more than the parent VOC, which is being treated (Mo et al., 2009b). Harmful intermediates could be the major impediments for field application of PCO technology. This issue of secondary intermediates was also pointed out by the Project Monitoring Committee. In addition to vapour phase intermediates, some partially oxidised semi-volatiles can deposit on the catalyst surface and may be released when catalyst is regenerated.

In the above context, the Ministry of Environment, Forests and Climate Change (MoEFCC) sponsored a project with objective to develop and demonstrate photocatalytic oxidation (PCO) technology for controlling VOCs at source and *in situ* ambient indoor air using nano-semiconductor catalysts (TiO_2) and ultraviolet (UV) radiation. The project was initiated in April 2012 and pilot testing and establishing the technology was one of the important objectives, so that the technology is brought to the level that it can potentially be used in the industry. A student Indramani Dhadha had extensively worked on this project leading to his PhD thesis. A major part of his thesis and research papers published have contributed to this report. M/s Aarti Industries Limited, Vapi, Gujarat was the participating industry which came forward to support the study at their premises and extend all assistance in pilot testing and provide necessary support for safety and field application.

It is expected that the harmful organics can be effectively converted into harmless water vapor (H_2O) and carbon dioxide (CO_2) through PCO technique. An Interim report was submitted in February 2014 during the meeting of Project Monitoring Committee (PMC). The PMC was satisfied with progress of the project.

The other issues (i) absorption of UV radiation to accomplish band gap energy requirement, (ii) estimation of reaction kinetics for PCO of VOCs as a function of time of operation and exposed surface area of catalyst, (iii) deactivation and regeneration of TiO₂ catalyst, (iv) develop and evaluate a photo catalytic device for controlling VOCs in indoor air (in various chemical environments), (v) model the interaction between indoor air and kinetics of VOC degradation and (vi) identify and quantify the intermediates of degradation (vapour and solid phase) to assess the exposure risk were duly addressed for making the technology full operational.

1.2 PCO Technology

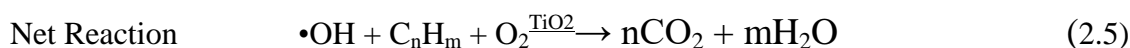
PCO with titanium and other semiconductor based catalysts has been extensively studied for VOC control (USEPA, 2011; Tejasvi et al., 2015; Dhada et al., 2015b). The mechanism of PCO at the surface of photocatalyst involves excitation of an electron (e⁻) in an electron-filled valence band (VB) by photo-irradiation to a vacant conduction band (CB), leaving a positive hole (denoted as h⁺) in the VB. The energy band gap between CB and VB in anatase phase of TiO₂ is 3.2 eV, which can be activated by UV radiation with a wavelength up to 387.5 nm (Shuang-shi et al., 2012). The excited electron and h⁺ lead to formation of hydroxyl radical (·OH) in presence of water vapour (Matsunaga et al., 2008). Being a strong oxidizing agent, ·OH converts organic compounds into simple products such as water vapour and CO₂ (Černigoj et al., 2007). Carp et al. (2004) provided an excellent review of PCO technology using TiO₂ as a catalyst. The remarkable fact about PCO is that it can be effective at ambient conditions in a hollow surface reactor without any significant pressure drop.

1.3 Factors Influencing PCO

Photocatalytic oxidation is a typical heterogeneous reaction process. It is influenced by many factors like type of catalyst, catalyst particle size, humidity, temperature, strength of photon energy etc. Each factor must be optimised for an effective PCO process. Some important factors influencing gas-phase TiO₂-PCO reactions are discussed below.

1.3.1 Choice of Catalyst

Several catalysts are developed for PCO applications. In general, the common photocatalysts are in the form of metal oxides or sulphides, i.e., TiO₂, ZnO, ZrO₂, SnO₂, WO₃, CeO₂, Fe₂O₃, Al₂O₃, ZnS and CdS (Hoffmann et al., 1995). The most common choices for photocatalysts are TiO₂ and ZnO. Ollis.(2000) assessed the photo-activity of several metal oxides for oxidation of hydrocarbon in gas phase and ranked them as: TiO₂ (anatase) > ZnO > WO₃. Among the available wide range of photocatalysts, most PCO studies (Salaices et al., 2004; Yen et al., 2010; Xiao et al., 2013) have used TiO₂ nano-particles as the UV radiation excitable catalyst because of catalytic activity, chemical stability, non-toxicity, relative inexpensiveness and availability of TiO₂ (Sakatani et al., 2006). Anatase phase of titania is widely used as this phase is the most photoactive (Fujishima and Zhang, 2006). The energy band gap between CB and VB in anatase phase of TiO₂ can be activated by UV radiation with a wavelength up to 387.5 nm (Benoit-marquié et al., 2000; Shuang-shi et al., 2012). The following major pathways of VOC oxidation have been suggested (Collins, 2012):



1.3.2 Characteristics of TiO₂ Coating

Photocatalytic gas-phase reactions are mostly carried out in the reactors having immobilized catalysts bound to a support surface (referred to as substrate). Various supports and immobilization methods for TiO₂ photocatalysis, such as electrophoretic deposition, spray coating, solvo thermal method, precipitation (co-) methods have been reported (Fernandez et al., 1995; Byrne et al., 1998; Carp et al., 2004). The substrates for the coating include conducting glass, stainless steel, titanium foil, tin coated glass, aluminium sheet (Carp et al., 2004; Dhada, 2008; Dhada et al., 2015a). Carp et al. (2004) have reported an excellent review of catalyst coating methods. Another route for in situ coating is through a combined physical and chemical transformation like sol-gel synthesis (Kim and Anderson, 1994). The sol-gel method has many advantages over other techniques such as purity, homogeneity, felicity, and flexibility in introducing dopants in large concentrations, stoichiometry control, ease of processing, control over the composition, and the ability to coat large and complex areas (Carp et al., 2004). The sol-gel process is widely used for depositing thin layer of catalyst (Han and Naeher, 2006; Yoon et al., 2006). Sol-gel is one of the most successful techniques for preparing nano size metallic oxide materials with high photocatalytic activities (Dzik et al., 2010).

Field emission-scanning electron microscopy (FE-SEM) technique is used for surface morphology and estimating film thickness. Keshmiri et al. (2006) reported the optimum thickness of sol-gel coating in the range of 10-50 μm . Tejasvi et al. (2015) used FE-SEM technique at various magnifications to investigate uniformity of TiO₂ coating, crack width

and width of pieces. The crack widths should be as small as possible to ensure the uniformity in the catalyst coating and for longer adhesion of the coating on the substrate which ensures greater wear and tear endurance. Energy dispersion absorption x-ray spectroscopy (EDAX) technique is used for the elemental analysis of coating of TiO₂ surface. The EDAX analysis gives the percentage elemental composition of the coating. This knowledge can be used for ascertaining presence of TiO₂ and other impurities in the coated surface. Atomic force microscopy (AFM) technique gives the root mean square surface roughness. For comparable surface areas, higher surface roughness will be more effective for PCO than the smooth surface. Dhada et al. (2015a) reported a surface roughness of coating as 1408 ± 95 nm.

1.3.3 Temperature

Temperature has an important role in gas-solid phase heterogeneous reactions. However, photocatalytic reactions are not sensitive to minor variations in temperature (Fox and Dulay, 1993). Photocatalytic degradation is more effective at a moderate temperature range than at an elevated temperature because the adsorption of reactants on the photocatalyst surface is difficult at a higher temperature range (Obee and Hay, 1997; Kim et al., 2002; Dhada, 2008). The optimum temperature range for PCO has been reported as 25-45°C where toluene has been observed to be more effectively reduced towards the lower end of the range (Kim et al., 2002).

1.3.4 Relative Humidity

During the process of photocatalysis, the h⁺ generated in the VB migrates to the catalyst surface and react with the adsorbed moisture to produce highly reactive species such as •OH. These species can participate in a host of redox reactions, which are highly effective in destruction of VOCs. The continuous consumption of •OH in PCO requires constant

replenishment to maintain catalytic activity. Water vapour can act as a constant supply of OH^- which is the precursor species of $\bullet\text{OH}$. Thus with increasing humidity the reaction rates are observed to be higher. A certain degree of humidity is necessary to maintain hydroxylation and to avoid the blockage of the TiO_2 surface by partially oxidized products (Ameen and Raupp, 1999; Maira et al., 2001). With increase in vapour content, the equilibrium can get disturbed and more water vapour molecules than the target organic compounds may be adsorbed on the catalyst surface (Carp et al., 2004). Additionally, water adsorption favours electron-hole recombination (Lichtin, 1996), which is not desirable. Al Momani. (2007) reported that relative humidity (RH) of 50% is an optimal humidity level for the O_3/UV degradation process.

1.3.5 Concentration of Pollutants

Kachina. (2008) has reported that at a constant reaction rate is attained with high concentration of pollutant, as catalytic sites become occupied so that a further increase in the pollutant concentration does not affect the actual catalyst surface concentration and results in a decreased relative pollutant conversion. The another plausible explanation put forward by Kachina. (2008) about the saturation behaviour of PCO is the relation between generation and migration of photo generated electron-hole pairs and their reaction with organic compounds. At low concentrations, the degradation rate increases linearly with the pollutant concentration as reaction dominates. However, at high concentrations of pollutant the generation of electron-hole pairs will become the rate determining step and the degradation rate increases slowly with concentration for a given illumination intensity (Kachina,2008). Intermediates generated during the PCO also affect the adsorption and oxidation rate of their parent compounds. A higher initial concentration will yield a higher concentration of adsorbed intermediates, which will affect the overall rate (Carp et al., 2004). Therefore, there is a need

to study the PCO with varying initial concentration and assess the changes in the degradation rate and rate constants.

1.3.6 Ultra Violet Irradiation

Ultraviolet radiation is important part of the photocatalytic process. The UV-C (wavelength from 200 to 280 nm) radiation could activate titania photocatalysts. However, only 4-5% of the solar energy reaching the ground level could be utilised in PCO when TiO₂ is used as photocatalyst (Yu-Zhang et al., 1994; Carp et al., 2004). Hence external UV source is required when TiO₂ is employed. The germicidal lamp (UV-C, 254 nm) and fluorescent black-light lamp (300-370 nm) have been commonly used (Obee and Hay, 1997; Benoit-marquié et al., 2000). Besides supplying the required energy for catalyst activation, the photons from UV light can also participate in direct photolysis reactions. These high energy photons are known to be effective in attacking the C—C bond and resulting in the subsequent degradation (Carp et al., 2004; Al Momani, 2007). The degradation rate of toluene was reported to be higher with a UV light of 254 nm than the toluene conversion irradiated with a UV light of 360 nm (Al Momani, 2007).

1.3.7 Photocatalyst Deactivation

Gas–solid photocatalytic activity has been observed to decrease with time, which is due to the decrease of active catalyst sites on the reaction surface (Sauer and Ollis, 1996; Ollis, 2000). Therefore, photocatalyst deactivation is a crucial issue in practical applications. Depending on the characteristic of the organic compounds, either reversible or irreversible deactivation was evidenced (Peral and Ollis, 1997; Piera et al., 2002). The catalyst may be deactivated by either the formation of surface intermediates with higher adsorption ability

than the target pollutant (reversible deactivation) or by sticky “large molecular weight” products that are difficult to decomposed or desorbed (irreversible deactivation).

1.3.8 Brunauer, Emmett and Teller (BET) Surface Area

The BET surface area is the area of the catalyst which actually participates in PCO process. The higher the BET surface area is, the higher the degradation rate will be (Dhada et al., 2015a). A BET surface area of 50 m²/g was reported by D’Hennezel et al. (1998) for commercially available P-25-TiO₂ particles and 32.53-102.3 m²/g is reported by Korologos et al.(2012) for TiO₂ doped with Ce.

From the discussion in section 2.2, it is stated that the TiO₂ based photocatalytic oxidation of VOCs in presence of UV-C light ($\lambda=254$ nm) at temperature 25°C to 45°C and RH 50 % is most effective method. Sol gel method of coating of TiO₂ with maximum BET surface area is an effective process to degrade the VOCs to CO₂ and H₂O.

1.4 Degradation Rate Constant and Regeneration

Degradation rate constant (k; per min per unit surface area of catalyst) of VOC shows the effectiveness of PCO technology. Dhada et al. (2015a) reported the k value ranging 1.07E-3 to 2.93E-3 min⁻¹cm⁻² for PCO of BTX. For PCO of benzene the degradation constant k has been reported as 0.115 min⁻¹ (Jacoby et al., 1996), 0.0324 min⁻¹ (He et al., 2014) and 7.6 E-5 min⁻¹cm⁻² (Tejasvi et al., 2015). Similarly for toluene, the degradation constant k has been reported as 1.25 min⁻¹cm⁻² (Korologos et al., 2012), 0.0321 min⁻¹ (Chen et al., 2011), 0.04-0.118 min⁻¹ (Kim et al., 2002) and 1.0E-3 min⁻¹cm⁻² (Tejasvi et al., 2015). VOC degradation rate decreases with elapsed operation time of reactor (Dhada et al., 2015b). Therefore it is

necessary to regenerate the catalyst after a certain time of operation of reactor for effective and long-term use of catalyst. It is important to consider the appropriate design value of degradation constant as it is a function of time. No earlier studies have focused on the degradation constant as a function of time.

1.5 Intermediates and Associated Risk

Intermediates generated from PCO of VOCs may block the active surface of catalyst (described in Section 2.2.7) and at the same time intermediates could be released in the indoor environment and can pose health risk to the occupants. These intermediates could be in vapour phase and adsorbed on the catalyst. The intermediates need to be identified and quantified. There have been several studies which have measured/suggested intermediates of benzene degradation (Jacoby et al., 1996; D’Hennezel et al., 1998; Zhang et al., 2006; Zhong et al., 2007; Han et al., 2008; Korologos et al., 2012; He et al., 2014) and toluene degradation (D’Hennezel et al., 1998; Boulamanti et al., 2008; Guo et al., 2008; Mo et al., 2009b; Korologos et al., 2012). Some studies (D’Hennezel et al., 1998; Mo et al., 2009b), based on identified intermediates, have proposed degradation pathways. There are only a few studies (e.g. Mo et al., 2009b) that have assessed the health risk of intermediates and that also only for toluene. There are no other studies on intermediates of other commonly present VOCs (e.g. ethylbenzene, p-xylene, m-xylene and o-xylene).

To accomplish the objectives described earlier, the overall work plan consists of three components: (i) Improving PCO Technology - laboratory scale study for reaction kinetics, catalyst degeneration and regeneration, (ii) Field application of technology and (iii) Risk characterization of exposure to intermediates. Figure 1.1 shows the summary of major tasks and adopted approach in this project.

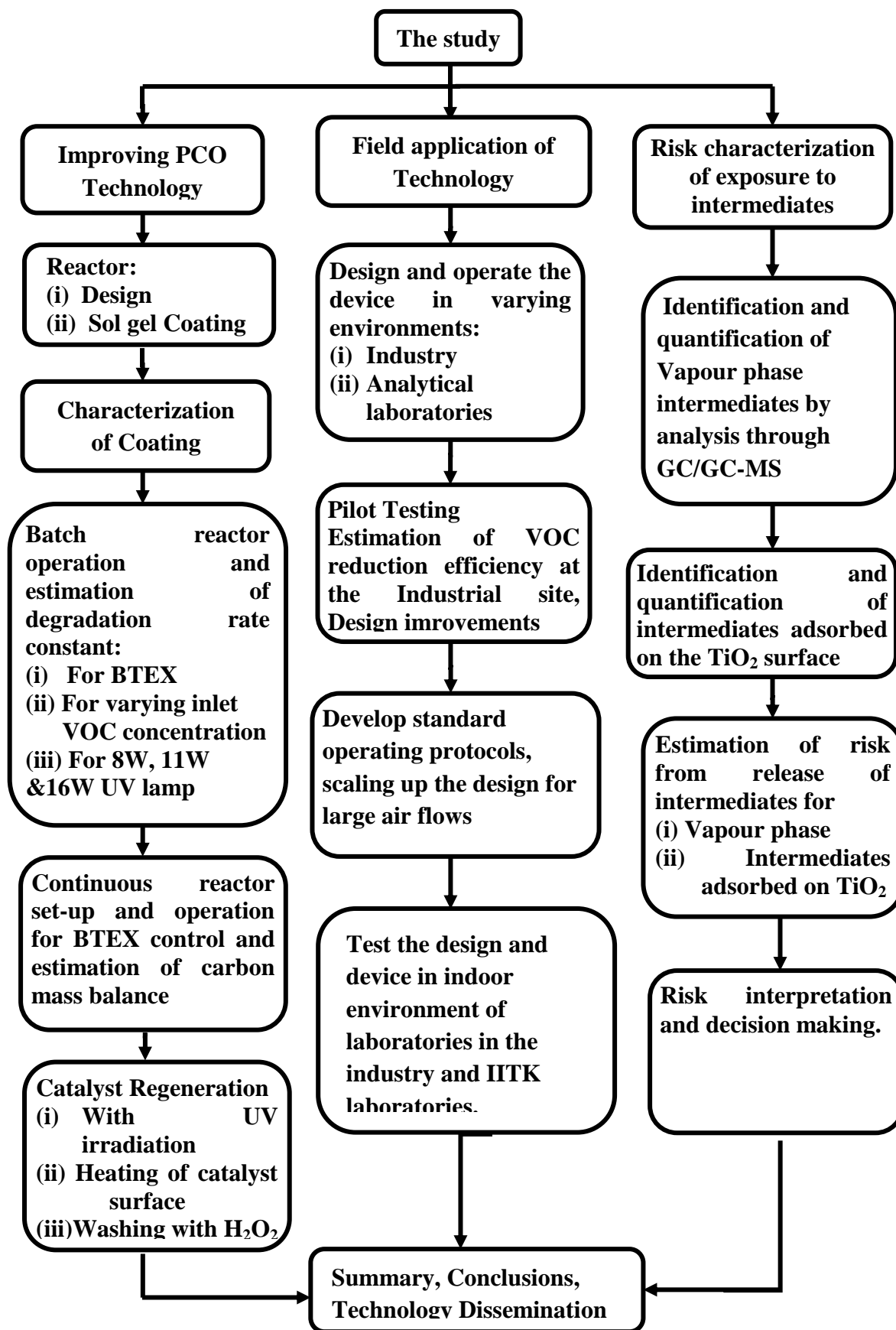


Figure 1.1: summary of major tasks and adopted approach

2

Materials and Methods

As summarized at the end of Chapter 1, this research has three components: (i) improving PCO technology; (ii) field application of technology; and (iii) risk characterization of exposure to intermediates.

2.1 Improving PCO Technology

This component of the study comprises fabrication of PCO reactor, TiO₂ coating, characterization of coating, laboratory scale reactor operation for estimating kinetics of VOC degradation and regeneration of catalyst surface. More details on TiO₂ coating, characterization and kinetics of degradation are presented in Dhada et al. (2015 b).

2.1.1 *Fabrication of Reactor*

TiO₂ coated borosilicate glass tube reactor (60 mm inner diameter and 270 mm length) was developed (Figure 3.1). The single reactor had effective volume=700 cm³, inner surface area = 524 cm² and it was equipped with digital temperature and relative humidity (RH) meter (Countrun, New Delhi) Both ends of reactor were sealed using air tight teflon (PTFE) caps, especially fabricated with the facility for injecting and withdrawing VOCs. UV-C transparent germicidal lamps of 8, 11 and 16Watts (15 mm outside diameter, 300 mm length, $\lambda=254$ nm, Sankyo Denki, Japan) were used as source of UV light. There was a provision to co-axially place one lamp inside the reactor. The length of the lamps ensured uniform illumination over the entire catalyst surface.



Figure 2.1: TiO₂ coated reactors with teflon caps

2.1.2 Preparation of TiO₂ Coating

All chemicals used in this study were of analytical reagent (AR) grade. Sol-gel process comprising hydrolysis, condensation and formation of thin TiO₂ film at low temperature was used for coating TiO₂ inside the reactor surface (Mo et al., 2009a; Collins, 2012). Tejasvi et al. (2015) experimented with eight solgel methods with some modifications and characterized the coatings for surface morphology, particle size, film thickness, band gap energy etc. and suggested an effective coating method, which was used in this study. Two sols (Sol A and Sol B) were prepared from a mixture of titanium tetra-iso-propoxide (TTIP; 98%; Spectrochem, Mumbai), di-ethanolamine (DEA; 99.5%; Merck, Mumbai), acetyl acetone (AcAc; 99.55%; Loba Chemicals), de-ionized water (H₂O) and ethanol (C₂H₅OH) at a molar ratio of 1:1:0:0:34 (Sol A) and 1:0:1:3:20 (Sol B) respectively. Sols A and B were mixed and ultrasonicated (Ultrasonicator; Eneritech, Mumbai) for 30 minutes to get the final sol-gel. For coating, the following procedure was followed; filling of the reactor with the sol-gel, emptying it gradually after 2-3 minutes, drying slowly at room temperature for 10 minutes, heating in a hot air oven at 120 °C for 10 minutes, transferring into a muffle furnace at 500

°C for 15 minutes followed by cooling at room temperature for 10 minutes. The entire process was repeated 15 times to obtain the optimal catalyst film of TiO₂ (Tejasvi et al., 2015).

2.1.3 Characterization of Coating

The following four tests were employed to examine adhesiveness and mechanical strength of the coating (Table 2.1): (i) finger-rubbing test, (ii) water and ethanol immersion test, (iii) cello tape peel-off test and (iv) scratch test. The coatings that passed the above tests were selected for experiments. Surface morphology, particle size, elemental analysis of prepared TiO₂ films and uniformity of catalyst distribution were analyzed with field emission-scanning electron microscopy (FE-SEM; Model: SUPRA 40VP, Make: Carl Zeiss NTS GmbH, Germany) and energy dispersive x-ray spectroscopy (EDAX; Model: FeTX3EDS Oxford, Inc). For obtaining average particle size, X-Ray diffraction (XRD Model: ISO Debye Flex1001) analysis was performed (Chromium target) and data were recorded from 15 degree to 90 degree. To obtain surface roughness and presence of impurities in catalyst coating, atomic force microscopy (AFM; Model: Pico SPM II, Molecular Imaging, AZ, USA) was carried out with scanning probe having resolution of fraction of nanometre. For determining the band gap energy, UV-spectrophotometry (50 Bio UV visible spectrophotometer, Varian, USA) was used. Film thickness profile of each sample was measured using profilometer (Tencor Alpha X-100). Brunauer, Emmett, and Teller (BET) surface area of the catalyst powder (obtained by scratching the thin films from the substrates) was estimated using SMART SORBS 92/93.

Table 2.1: Adhesion tests

Tests	Description
Finger-rubbing test	The coated substrates were checked by rubbing finger on the surface. If the catalyst comes out of the surface then coating is ineffective.
Water and ethanol immersion test	The coated substrate was immersed in water and ethanol separately and shaken. The turbidity of the solution was observed which was caused as the catalyst gets separated out from the substrate surface.
Cello tape peel-off test	The coating was checked using an adhesive tape. Cello tape was applied to the surface and then was peeled-off. The coating in which the catalyst was coming out of cello-tape peel was rejected.
Scratch test	The coated surfaces were scratched using scalpel. The surfaces easily losing the coated catalyst were rejected.

2.1.4 Laboratory Reactor Operation

An experimental set-up for operation of continuous reactor was designed (Figure 2.2)

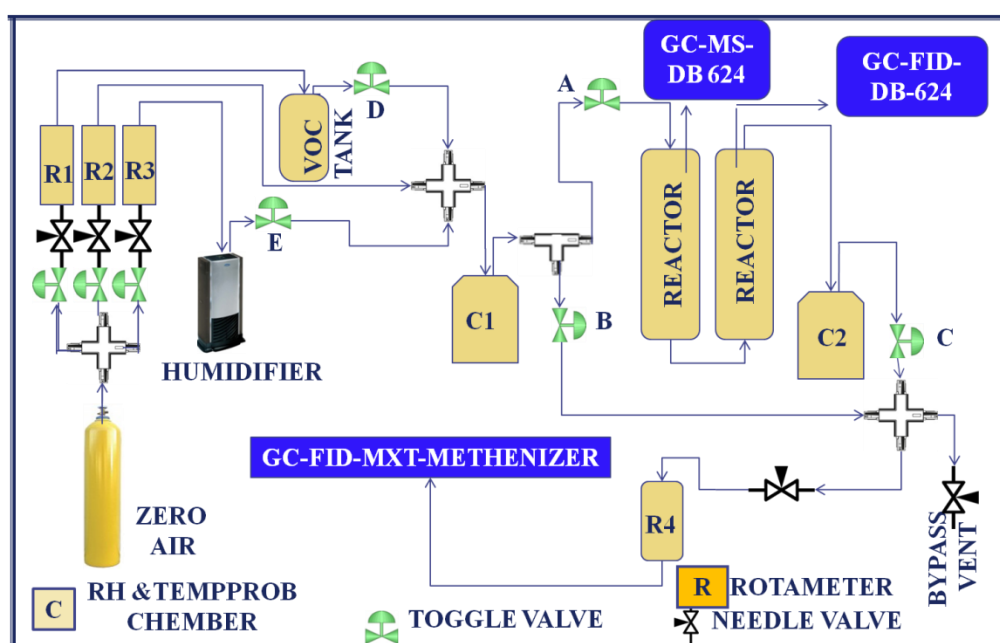


Figure 2.2: Schematic of experimental set up for continuous operation of photoreactor

The zero air was passed through toggle valves, rotameters, VOC tank, humidifier and mixing chamber (Figure 2.2) which produced inlet VOC stream. For measuring the inlet concentration, the VOC stream was allowed to reach Gas Chromatograph (GC) through toggle valve B and rotameter R₄. For measuring outlet concentration, VOC stream reaches GC through toggle valve (A), reactor, mixing chamber (C₂) and rotameter R₄. The GC used in this study (Buck Scientific Model 910, USA) was equipped with Restek MXT volatile column (0.53 mm ID, 30 m length, 2 µm film thicknesses) with a photo ionization and flame ionization detectors connected in series. For each experiment, the reactor was operated continuously for a period of 160 minutes, with a retention time of 7.0±0.25 minutes, RH 42.2±3.2 % and temperature 30.1±0.7 °C.

After the VOC concentration at the inlet and outlet of the reactor was identical and stabilized, the UV lamp was turned on. A number of experiments were performed by varying VOCs concentration (Table 2.2); at each concentration, the experiments were repeated three times.

Table 2.2: Inlet VOC concentrations considered for this study

Compounds	Individual analysis Retention time = 7.0±0.25 min	
	Inlet Concentration (mg/m ³)	
Benzene	High	376±18
	Moderate	120±10
Toluene	High	330±17
	Moderate	214±14
Ethylbenzene	High	360±19
	Moderate	122±08
p, m-Xylene	High	330±16
	Moderate	132±11
o-Xylene	High	335±19
	Moderate	193±10

Concentrations were measured at different time interval (20, 40, 60, 80, 100, 120 and 140 minutes interval) to understand the kinetics of degradation and estimate degradation rate constants, which can be utilized in design of VOC control device for field application. In outlet stream, carbon dioxide was also measured first by converting it to methane (CH_4) (using a methanizer) and then measuring CH_4 on FID.

2.1.5 Regeneration of Catalyst

After certain time of operation, performance of catalyst can deteriorate as the surface gets blocked with adsorbed intermediates. The catalyst regeneration is an important step and requires a definite method/approach. Three methods of catalyst regeneration (described below) were attempted to arrive at the effective catalyst regeneration methodology.

(i) Irradiating with UV light

After exhaustion of catalyst, the coated surface of reactor was regenerated through irradiation with UV light for 720 minutes; this was accomplished via oxidation of the compounds adsorbed on the catalyst surface. Then the regeneration efficacy was assessed by examining the extent of recovery of degradation rate. The degradation rates (before and after regeneration) were compared to know the extent of recovery of catalyst activity. The 8W, 11W and 16WUV lamps were used for assessing the regeneration potential.

(ii) Washing with H_2O_2

After each cycle of catalyst exhaustion, the coated surface of reactor was regenerated by washing the exhausted catalyst surface with aqueous solution of 30 % (wt) H_2O_2 . The degradation rates (before and after regeneration) were compared to know the extent of

recovery of catalyst activity. The amount of H₂O₂ used was 95, 191, 286 and 382 ml/m² of catalyst surface area.

(iii) Heating in muffle furnace

After each cycle of catalyst exhaustion of the reactor, the coated surface of reactor was regenerated through heating the catalyst surface at 450°C in a muffle furnace for 15 minutes. The degradation rates (before and after regeneration) were compared to know the extent of recovery of catalyst activity.

2.2 Field Application of Technology

A proto type device (Figure 2.3) consisting of seven numbers of reactors (described in section 3.1.1) in series was fabricated and installed in three indoor environments (described later) to examine field worthiness of technology. Through the help of flow regulator and rotameter, the flow rate of VOC laden stream (into the device) was set to desired level (Table 2.3). The Total Volatile Organic compounds (TVOC) concentration was measured through a TVOC analyzer (ppb RAE 3000, Honeywell, CA 95134-1708 USA) at the inlet and outlet of the device. The time totalizer indicated the running time period of device. The temperature and RH was measured at the inlet and outlet of the device.

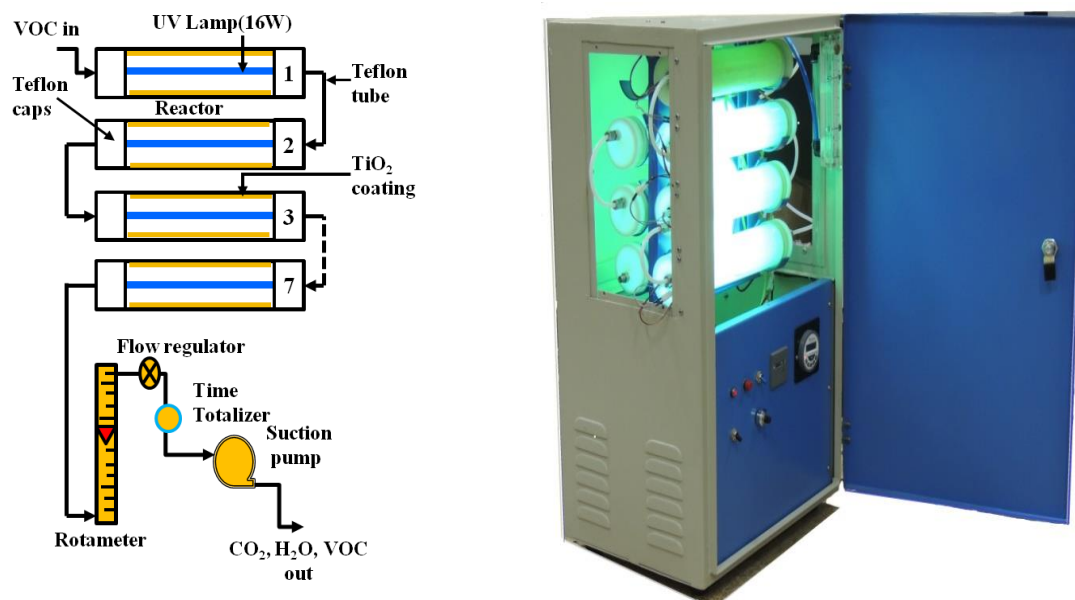


Figure 2.3: Full-scale VOC control device (schematic)

The fabricated device was evaluated through three different studies, Case-1, Case-2 and Case-3. Table 2.3 presents summary of these three case studies including type of indoor environment, VOC(s) being treated and its concentration, flow rate and duration of operation of device. The temperature and RH during the experiments were $22.4 \pm 2.3^\circ\text{C}$ and $57 \pm 3\%$.

Table 2.3: Description of case studies, concentration of VOCs and physical parameters

Case study	Indoor environment and VOC(s)	Size of room	Flow rate (lpm)	Period of operation (minutes)	Inlet TVOC concentration (ppm)
Case 1 [§]	Laboratory using benzene as solvent	8.6m × 6.1m × 3.7m	7	490	76-160
Case 2	Conference room of a solvent Industry producing MCB,DCB and TCB*	3m × 2.8m × 3m	4	95	62-81
Case 3	Large Chemistry laboratory using dichloromethane, methanol, ethyl acetate, acetone, hexane	12.2m × 12.2m × 3.7m	7	480	67-250

[§]study includes intermediates of benzene photo degradation and their health risk assessment

*MCB: Mono-chlorobenzene , DCB: Di-chlorobenzene, TCB: Tri-chlorobenzene

2.2.1 Case-1: Laboratory Using Benzene as Solvent

For Case-1, the intermediates (of benzene degradation) adsorbed on the surface of TiO₂ catalyst were identified on GC-MS and quantified on GC. For quantification of solid phase intermediates, identically coated glass chips (same as catalyst surface of device) of total area 3 cm² (Figure 2.4) were kept inside the device. In other words, the chips act as surrogate of the reactor surface and that of exhausted catalyst. After completion of operation of reactor, the chips were taken out and extracted with methanol for identifying and quantifying the intermediates adsorbed on the catalyst. It may be noted that the catalyst when regenerated by heating will emit the same compounds which are adsorbed on the chip. The chips were immersed in 15 ml methanol and ultrasonicated (Fast Clean, India) for 30 minutes. Extracted compounds (in methanol) was filtered through 0.45 µm syringe filter (Millex-HV, PVDF) and concentrated to 1.5 ml with the help of Turbo Vap (Turbo Vap-II, Caliper Life Science) by purging N₂ gas at 23°C. Then 0.4µl of extracted concentrated sample was injected in to the GC through 1µl syringe (Hamilton Bonaduz) for quantification of solid phase intermediates.



Figure 2.4: TiO₂ coated chips for analysis

2.2.2 Case-2: Conference Room of a Solvent Industry Using Monochlorobenzene (MCB), Di-chlorobenzene (DCB) and Tri-chlorobenzene (TCB)

The device was installed in the conference room of an industry producing, storing and handling organic solvents (MCB, DCB and TCB) to remove the VOCs (Figure 2.3). The details of experiment are given in Table 2.3. Initially the device was run without switching on the UV lamps till the inlet and outlet concentration becomes same. Then the UV light was turned on and the TVOC concentrations at inlet and outlet of device were measured at every 2 minute interval. The temperature and RH during the experiments were $22.4\pm 2.3^{\circ}\text{C}$ and $57\pm 3\%$.

2.2.3 Case-3: Chemistry laboratory using multiple VOCs (Dichloromethane, Methanol, Ethyl acetate, Acetone, Hexane)

The device was installed in a large chemistry laboratory of an academic institute using dichloromethane, methanol, ethyl acetate, acetone, and hexane. The details of experiment are given in Table 2.3. Initially the device was run without switching on the UV lamps till the inlet and outlet concentration reached the same level. Then the UV light was turned on and the TVOC concentrations at inlet and outlet of device were measured. The temperature and RH during the experiments were $27.5\pm 2.3^{\circ}\text{C}$ and $57\pm 3\%$.

2.3 Risk Characterization of Exposure to Intermediates

2.3.1 Identification and Quantification of Intermediates of Ethylbenzene, Xylene and Toluene (EXT)

The reactor was filled separately with EXT and it was operated as a batch reactor. The initial concentration of EXT taken in the batch reactor for identification and quantification of intermediates were high compared to the levels observed in indoor air (Table 2.4; column 2) so that measurable amounts of intermediates are obtained.

Table 2.4: VOCs studied for intermediates

VOC	Initial VOCs concentration (mg/m ³) for batch study to identify and quantify intermediates	Realistic indoor VOCs concentration (µg/m ³) for treatment and risk assessment of intermediates*
Ethylbenzene	180	220
p,m-xylene	190	260
o-xylene	130	260
Toluene	170	320

*Highest indoor air concentration reported earlier (Brickuset al., 1998; Sexton et al., 2004; Zhu et al., 2005; Weisel et al., 2008)

Samples were drawn at 40, 80, 120, 160, 200 minutes from the batch reactor so that the majority of intermediates are formed and quantified as a function of time. The experiment was repeated three times. The intermediates of EXT adsorbed on the catalyst surface were identified on GCMS and quantified on GC as per the extraction procedure described in sections 2.2.1. For vapour phase intermediates, samples (1 ml for each analysis) were drawn using a 5 ml gas tight syringe (SGE, Restek) and injected into GC-FID (Clarus 500, Perkin Elmer) which was equipped with fused silica capillary column SPB-624 (60m×0.25 µm×0.4 µm; Supelco make). The EXT

degrade through formation of benzene or toluene (Mo et al., 2009b; Dhada et al., 2015a) and therefore the GC was calibrated for previously reported intermediates of benzene and toluene [i.e. n-hexane, benzaldehyde, phenol, pentane, crotonaldehyde, benzylalcohol, cyclohexane, cresol, benzoic acid, hydroquinone, benzene, toluene, xylenes, ethylbenzene, methanol (Jacoby et al., 1996; Cao et al., 2000; Guo et al., 2008; Han et al., 2008; Sleiman et al., 2009; Mo et al., 2009b; Farhanian and Haghghat, 2014) at four levels (5, 50, 100, 500 ppm). The temperature programming for GC was: 40°C, 5 min hold- ramp@10°C/min up to 200°C, 5min hold - ramp@10°C/min up to 240°C, 1 min hold.

The realistic concentration of EXT in indoor air (Table 2.4; column 3) is much less than the initial concentration used in the batch reactor. For demonstrating the risk assessment, it is assumed that a device consisting of seven reactors in series treats the reported concentration of EXT at a flow rate of 7 lpm for a laboratory of volume 195 m³ (Figure 2.3).

2.3.2 Exposure to Released Intermediates of BTEX: Risk Assessment

The intermediates of BTEX (see sections 5.1-5.2) may pose risk to the occupants of buildings. To demonstrate the risk, it is assumed that a laboratory has installed the device and occupants could be exposed to the intermediates. The risk of exposure can be assessed through hazard index (HI) (Asante-Duah, 1998) and cancer risk. Specifically, the HI has been estimated for permanent staff (PS) who works in laboratory for 35 years.

The total chronic hazard index (HI) can be calculated as

$$HI = \sum_{i=1}^n \frac{CDI_i}{RfD_i} \quad (3.1)$$

Where CDI_i is chronic daily intake for the i th VOC and RfD_i is the reference dose (mg / kg-day) for the i th VOC

The CDI is calculated as per the following formulation

$$CDI = \frac{(CA \times IR \times ABS_s \times ET \times EF \times ED)}{(BW \times AT)} \quad (3.2)$$

Where CA: Chemical/VOCs concentration in air (mg/m^3)

IR: Inhalation rate (0.83m³/h for adult)

ABSs: % chemical/VOCs absorbed into the blood stream (taken as 100%)

ET: Exposure time (8h/day)

EF: Exposure frequency (261days/year; 5working days a week)

ED: Exposure duration (35 years)

BW: Body weight (70kg)

AT: Averaging time (period over which exposure is averaged: 70 years× 365days/year)

The value of parameters given in parenthesis have been adopted from Asante-Duah (1998).

3 Improving PCO Technology: Designing, Coating and Regenerating Catalyst

This chapter addresses impediments in technology application by specifically focusing on TiO₂ coating, estimation of reaction kinetics (as a function of time of operation), designing a continuous reactor, and deactivation and regeneration of TiO₂ catalyst. The following five VOCs were studied: benzene, toluene, ethylbenzene (ETB), p,m-xylene (all together referred to as BTEX).

3.1 Characterization of Coatings

Effective coating of catalyst is of paramount importance which can be examined by characterizing the coating surface. The FE-SEM image of the coated samples showed the surface morphology and the particle size of the TiO₂ (Figure 3.1-a and 3.1-b). This analysis concluded that (i) TiO₂ particles were uniformly distributed throughout the surface and (ii) particles size of TiO₂ was 10.2±1.43 nm (close to 14 nm reported by Koci et al., (2009). With a smaller particle size, the number of active surface sites increases and so does the surface charge carrier transfer rate in the photo catalysis. By comparing the XRD pattern of the sample (Figure 3.2) with standard XRD pattern of TiO₂anatase phase (Source: PCPDF software; File No.: 711169), it can be stated that the crystalline phase of coated TiO₂ particles was anatase.

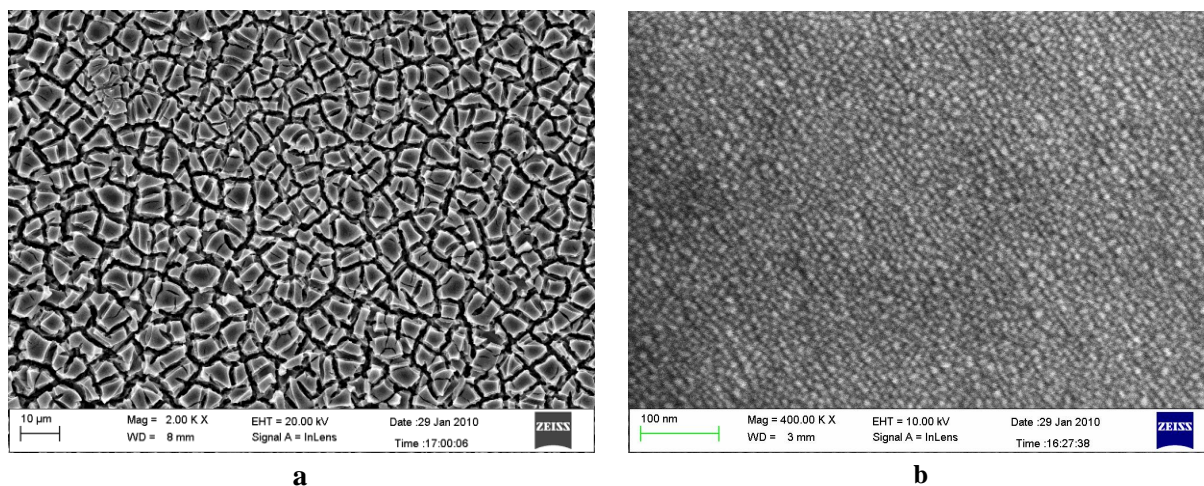


Figure 3.1: FE-SEM image showing the surface morphology for TiO₂ nanoparticles (a) at 10μm (b) at 100 nm resolution (Dhada et al., 2015 b)

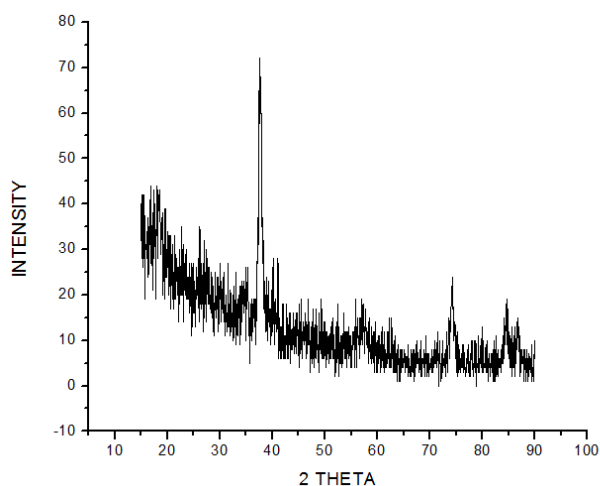


Figure 3.2: XRD pattern: 2θ v/s intensity graph

The EDAX analysis (Figure 3.3 and Table 3.1) of the coated samples established that TiO₂ was the main constituent of the coating. The fraction of Titanium is 51.83±0.87 (wt/wt %) and the fraction of the Oxygen is 46.19±0.89 (wt/wt %). For TiO₂ alone, the atomic ratio of Ti and O

should be 1:2, however, the obtained ratio is 1:2.66. This is due to the fact that O₂ will be associated with other metals present in the catalyst.

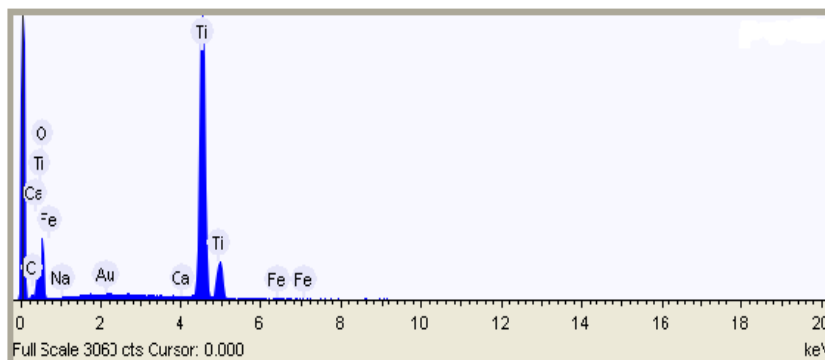


Figure 3.3: EDAX spectra of TiO₂ coated thin film

Table 3.1: Composition of different elements in TiO₂ coated thin film

Element	Weight % $\pm\sigma$	Atomic %
Titanium (Ti)	51.83 \pm 0.87	26.69
Oxygen (O)	46.19 \pm 0.89	71.23
Carbon (C)	0.77 \pm 0.31	1.58
Sodium (Na)	0.27 \pm 0.12	0.28
Calcium (Ca)	0.12 \pm 0.06	0.07
Iron (Fe)	0.11 \pm 0.10	0.05
Gold (Au)	0.72 \pm 0.27	0.09

The AFM analysis (Figure 3.4-a) of TiO₂ particles estimated root mean square surface roughness as 1408 ± 95 nm. The obtained surface roughness would provide a higher exposed surface area to VOCs than by a smooth surface. It may be noted the phase image (Figure 3.4-b) showed that the thin film of TiO₂ was composed of uniform and homogenous particles.

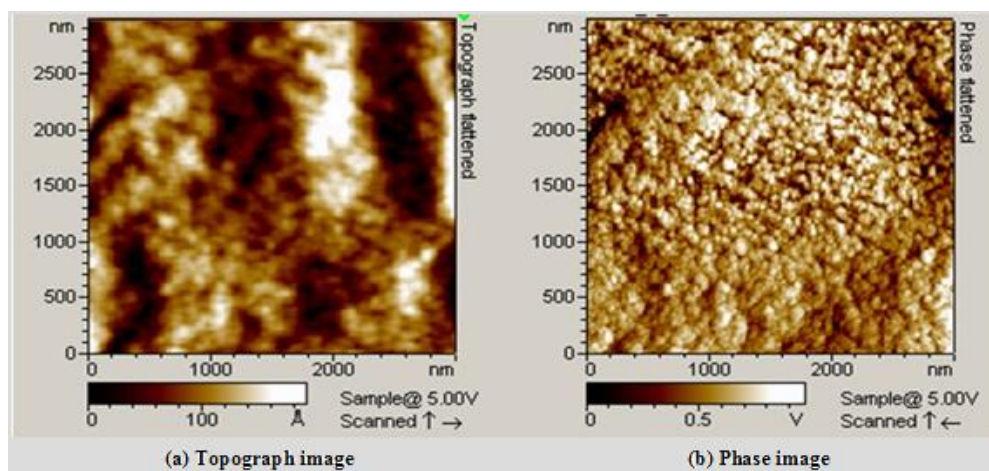


Figure 3.4: AFM image of TiO₂ coated thin film (Dhada et al., 2015 b)

The absorbance spectra of the TiO₂ coating (Figure 3.5(a)) shows that almost all UV radiation below 350 nm (approximately) was absorbed by the catalyst and for UV radiation above 400 nm (approximately) the absorbance was reduced to 0.70. The transmittance spectra for TiO₂ coated glass substrate (Figure 3.5(b)) indicated that transmittance through the coated surface was very small for radiation wavelength below 400 nm (i.e. less than 20%). Therefore, it is concluded that lower wavelengths UV radiation is absorbed on the TiO₂ coating. The band gap energy of TiO₂ particle was estimated 3.25 eV (Figure 3.5(c)) using Planck Einstein equation ($E = h \times c / \lambda$, $h =$ Planck's Constant, $c =$ Speed of Light, $\lambda =$ wavelength in nm, $E =$ energy in eV) (Nagar, 2010), which was close to the reported value of 3.23 eV for the anatase phase of TiO₂ particles (Mo et al., 2009a).

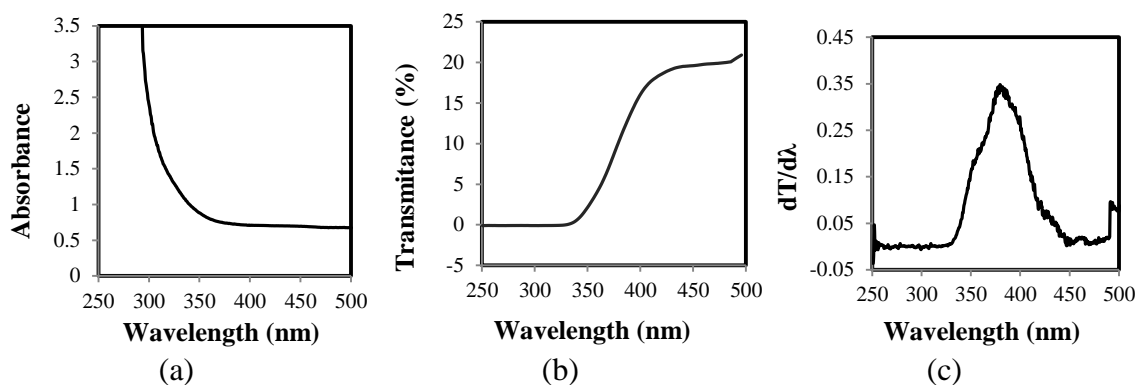


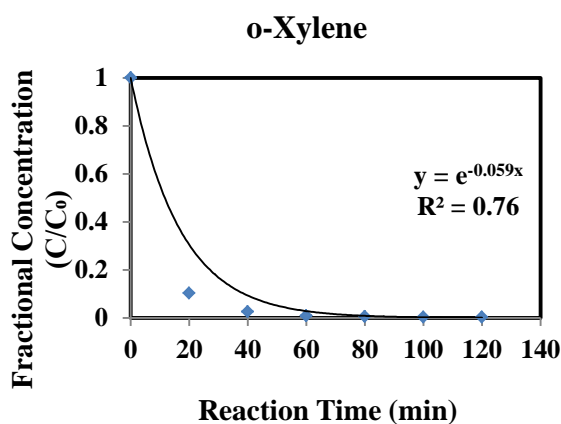
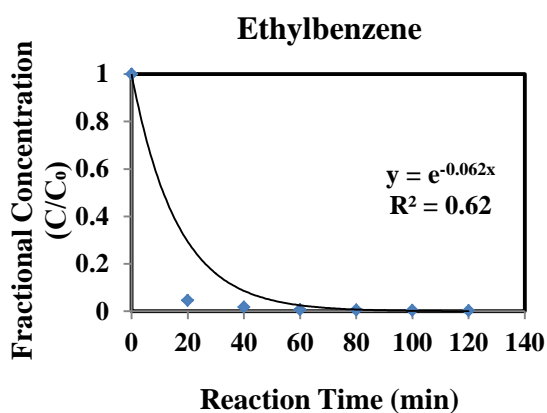
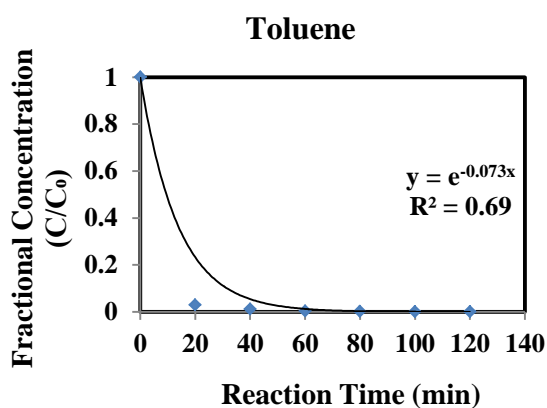
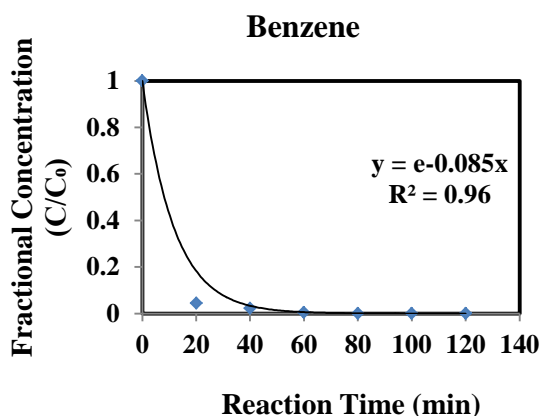
Figure 3.5: UV spectra of coating and band gap; (a) absorbance spectra, (b) transmittance spectra and (c) determination of the band gap for TiO₂ coated glass substrate (Dhada et al., 2015 b)

In profilometry analysis, the obtained average thickness of coating was 23.9 μm , which is in the range of thickness (10-50 μm) reported by Keshmiri et al. (2006). The BET surface area of catalyst powder that was obtained by scratching the thin films from the substrates was 98m²/g. Based on the above analyses, it can be stated that effective TiO₂ particle coating has been obtained in terms of surface morphology, particle size, surface roughness, coating thickness and photo-activity for the PCO. The above tests and analyses have ensured effective coating and to enhance the technology such procedures should be followed and standardized for catalyst coating.

3.2 Kinetic of VOCs Degradation in Batch Reactor

The TiO₂ coated reactor was used to study the kinetics of the PCO of individual VOCs with the UV lamps of 8, 11 and 16 Watts in a batch process. The degradation rate for VOCs for different UV lamp wattage followed first order kinetics (Figure 3.6; shown only for 8 Watt UV lamp). The values of degradation rate constants (k) for the above three wattage for an operation period of 120 min are shown in Table 3.2. Rate constant increase with wattage of the UV lamp and is

maximum for benzene. The estimated k values can be used to design a continuous reactor system for removal of VOCs at a desired efficiency. Tejasvi et al. (2015) have reported a k value of $0.765 \text{ min}^{-1}\text{m}^{-2}$ for benzene and $1.07 \text{ min}^{-1}\text{m}^{-2}$ for toluene with sunlight as the only source of UV radiation. The degradation rates determined in this study are: 0.089 min^{-1} (i.e. $1.69 \text{ min}^{-1}\text{m}^{-2}$ for 16W UV) for toluene and 0.094 min^{-1} (i.e. $1.79 \text{ min}^{-1}\text{m}^{-2}$) for benzene and these rates are comparable with other studies; Chen et al. (2011) (0.0321 min^{-1} for toluene), Kim et al. (2002) ($0.04 - 0.118 \text{ min}^{-1}$ for toluene) and Jacoby et al. (1996) (0.115 min^{-1} for benzene).



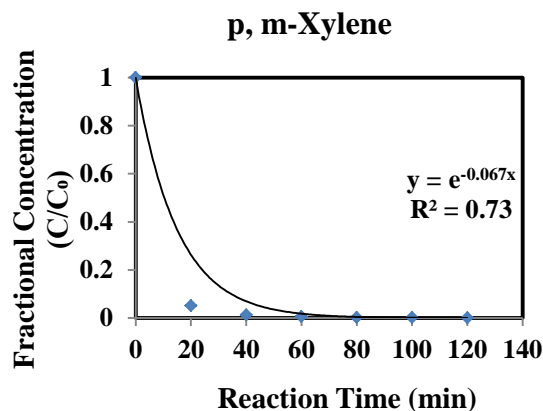


Figure 3.6: PCO of various VOCs: BTEX in batch reactor in presence of 8W UV lamp

Table 3.2: Degradation rate Constants (k) for VOCs in $\text{min}^{-1}\text{m}^{-2}$ of TiO_2 surface area (estimated from first two hour of operation of reactor)

Compound	Initial concentration (mg/m^3)	Degradation rate constants (k) ($\text{min}^{-1}\text{m}^{-2}$)		
		8W UV lamp	11W UV lamp	16W UV lamp
Benzene	150±30	1.65±0.08	1.63±0.03	1.79±0.05
Toluene	161±26	1.44±0.05	1.49±0.06	1.69±0.07
ETB	170±21	1.21±0.04	-	-
p, m-Xylene	181±25	1.26±0.07	1.35±0.08	1.45±0.03
o-Xylene	120±27	1.14±0.03	-	-

Degradation rate as function of duration of reactor operation

One reactor for each VOC was operated successively (without regeneration) for 0-1, 1-3, 3-5, 5-7, 7-9, 9-11, 11-13.5 hours, and the degradation rate was examined (Figure 3.7; as an example of benzene). It is important to note that in each successive experiments, the degradation rate constant for each compound progressively decreased, due to deactivation of catalytic surface with time (Table 3.3). This is possibly due the formation of highly adsorbed intermediates during the PCO of VOCs that leads to an abrupt decrease in the number of active sites during the

reaction on catalyst surface. Cao et al. (2000) have reported that catalyst surface is gradually occupied by irreversible chemisorbed intermediates, which retard the reaction kinetics.

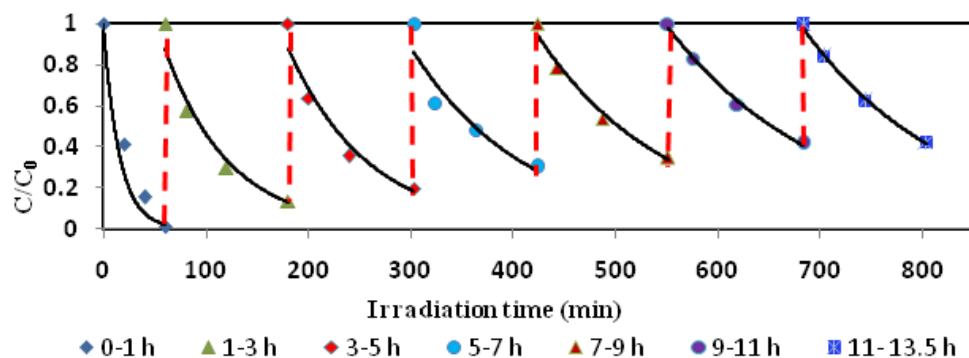


Figure 3.7: Variation in degradation kinetics over time for PCO of benzene in presence of 8W UV lamp (Dhada et al., 2015 b)

Table 3.3: Degradation rate constants (k) of VOCs in $\text{min}^{-1}\text{m}^{-2}$ of TiO_2 surface area over time

Reactor operation time(hr)	Degradation rate constant(k ; $\text{min}^{-1}\text{m}^{-2}$)							
	Benzene ($C_i=211\pm 21\text{ mg/m}^3$)		Toluene ($C_i=162\pm 18\text{ mg/m}^3$)		p,m-Xylene ($C_i=153\pm 14\text{ mg/m}^3$)		Ethyl benzene ($C_i=177\pm 19\text{ mg/m}^3$)	o-xylene ($C_i=143\pm 16\text{ mg/m}^3$)
	8W UV	16W UV	8W UV	16W UV	8W UV	16W UV	8W UV	8W UV
1	1.7 ± 0.09	1.79 ± 0.05	1.49 ± 0.06	1.69 ± 0.07	1.32 ± 0.03	1.45 ± 0.04	1.24 ± 0.02	1.16 ± 0.06
3	1.50 ± 0.04	1.74 ± 0.06	1.39 ± 0.22	1.65 ± 0.04	1.22 ± 0.14	1.4 ± 0.05	1.17 ± 0.13	1.12 ± 0.03
5	1.31 ± 0.15	1.71 ± 0.03	0.93 ± 0.31	1.39 ± 0.02	0.93 ± 0.11	1.05 ± 0.06	0.86 ± 0.09	0.81 ± 0.12
7	0.88 ± 0.07	1.66 ± 0.07	0.82 ± 0.25	1.03 ± 0.08	0.81 ± 0.08	0.84 ± 0.04	0.78 ± 0.04	0.76 ± 0.05
9	0.74 ± 0.09	-	0.71 ± 0.09	-	0.7 ± 0.12	-	0.68 ± 0.07	0.66 ± 0.08
11	0.69 ± 0.03	-	0.63 ± 0.05	-	0.62 ± 0.03	-	0.61 ± 0.07	0.57 ± 0.04
13.5	0.65 ± 0.05	-	0.60 ± 0.06	-	0.59 ± 0.02	-	0.56 ± 0.05	0.56 ± 0.03

C_i : Initial VOC concentrations

Degradation rate constant for toluene decreased much faster than other VOCs, possibly due to the formation of highly adsorbed species like benzoic acid and benzaldehyde (Rafael and

Cardona-martõ, 1998; Blount and Falconer, 2001). There are two isomers of benzaldehyde formed during the PCO of toluene: one form of benzaldehyde oxidized quickly and does not harm the catalyst, while another form of benzaldehyde with less reactivity remains on the reaction surface (Rafael and Cardona-martõ, 1998; Blount and Falconer, 2001). Benzoic acid is another intermediate which strongly adsorbs on the reaction surface of catalyst and causes its deactivation. The major intermediates that form during the PCO of benzene are phenol, which is accompanied by hydroquinone and 1,4-benzoquinone (D'Hennezel et al., 1998). Dhada. (2008) reported that intermediates formed during the PCO of ethylbenzene and xylenes are toluene and benzene. Thus degradation of ethylbenzene and xylenes will also pose problem of deactivation because benzene and toluene are the intermediates of ethylbenzene and xylenes.

Since the degradation rate is not constant over time, it poses a challenge as to what value of k should be used in designing and how frequently the catalyst must be regenerated; these issues have been discussed later in the text.

3.3 Regeneration of Catalyst

Three different techniques were employed to regenerate the catalyst to remove/oxidize the deposited organics to CO_2 and water. These techniques are (i) heating of reactor at $450\text{ }^\circ\text{C}$ for 15 minutes (ii) irradiation of surface with 16W UV lamp (Jeong et al., 2004) and (iii) washing of surface with a strong oxidizing agent H_2O_2 (Mohan., 2009). The regeneration potential for the above three techniques is shown in Figure 3.8 in terms of regenerated rate constant k

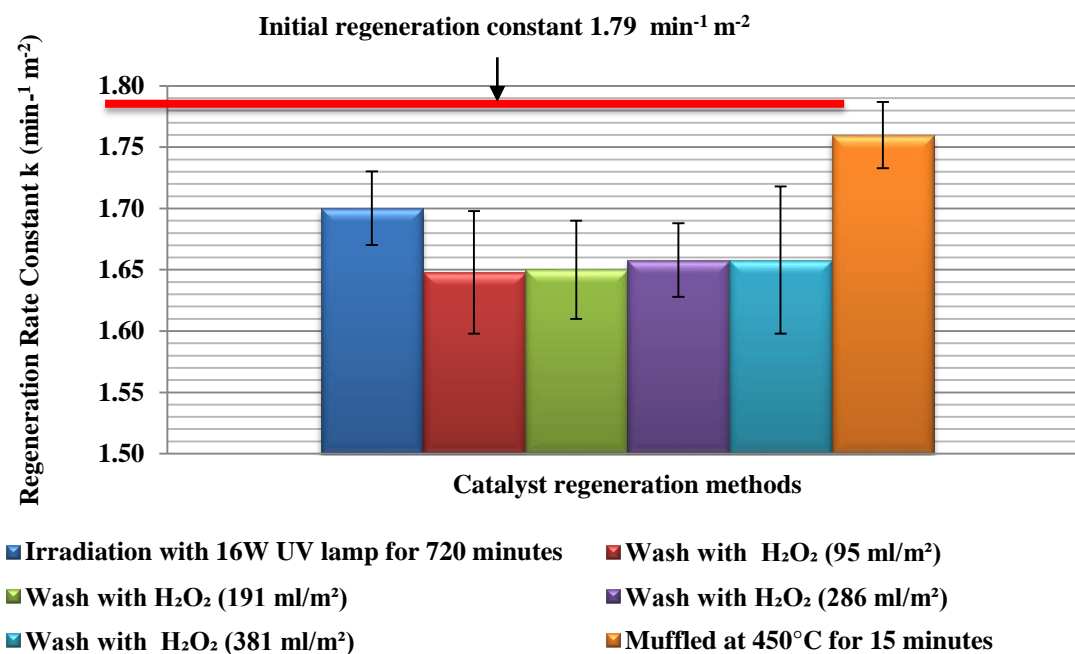


Figure 3.8: Catalyst regeneration methods (for PCO of benzene) (Dhada et al., 2015 b)

As expected, heating regenerates the catalyst fully as all organics (parent compound and intermediates) were evaporated and/or oxidized at 450°C and surface was regenerated to its original value. The second promising method is continuous irradiation by a 16W lamp (8 and 11 W UV lamp did not show appreciable regeneration) for 720 minutes so that all adsorbed organics are oxidized; the k values were regained to 95%. Although to a lesser extent (92%), the catalyst can be regenerated by washing it with 30% H_2O_2 . It was observed that if H_2O_2 is recycled, its strength will reduce and some H_2O_2 will be lost with time. With time, the recycled H_2O_2 will have to be made-up with fresh H_2O_2 . It may be stated that regeneration by heating was done over 100 times and it was seen that the catalyst was almost fully regenerated every time. The repeated regeneration of catalyst does affect its surface as seen from SEM image (Figure 3.9; after over 100 regenerations). However, in all experiments, the regenerated surface continued to regain

original degradation constant (k) for VOCs. It signifies that regenerated catalyst can be used without any modification or recoating for a reasonable time and one may consider either recoating the surface or discarding the used catalyst after about 100 regenerations.

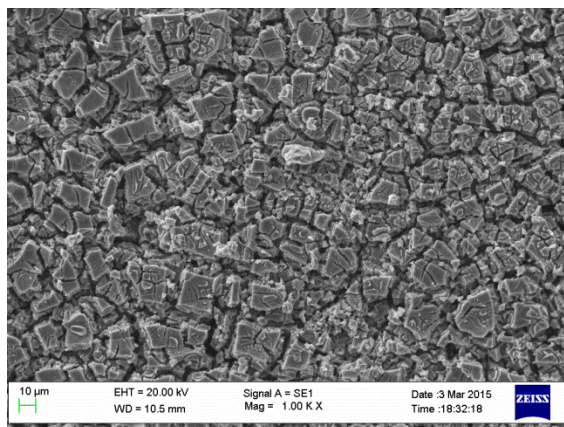


Figure 3.9: FE-SEM image showing the surface morphology for TiO₂ nanoparticles at 10 μm after 100 times of regeneration

3.4 Discussion

This study has specifically discussed the challenges and impediments that have prevented the TiO₂-based PCO technology from becoming commercially viable and widely accepted. Proper TiO₂ coating is of paramount significance. Nagar (2010) and Tejasvi et al. (2015) have optimized the method of coating and standardized it based on characterization in terms of structural continuity, surface roughness, surface impurities, strong surface attachment and particle size using AFM, XRD, FE-SEM, and EDAX analyses. It is important that the standardized coating technique must be followed in preparing the reactor. The particle size of TiO₂ in nano size is important for availability of large active surface area (around 100 m²/g) of catalyst which should reduce size of the reactor and the pressure drop. Any small error in coating and improper size of

TiO₂ particles can dramatically impact the performance of catalyst. It has been seen that higher wattage of UV lamp degrades the VOCs at much faster rates. It needs to ensure that an UV-C radiation is produced in the wavelength range 387.5nm and below.

The important design parameter for VOC removal is the degradation rate constant. Since degradation pathways for different VOCs are variable, so will be the degradation rate. This study clearly suggests the degradation rate for higher wattage of UV lamp is more (see Table 3.2) and this provides an opportunity to optimize wattage of UV lamp for field application.

While trying for stable performance of the reactor, the important challenge was to handle continuous deactivation of the catalyst which adversely affected the degradation rate. An incorrect value of k (which is decreasing with time of operation) results in long-term poor performance. For example, the k value for freshly coated TiO₂ can reduce by 10% in seven hours of operation (for 16W UV) and for 8W it can reduce by 60% in 13.5 hours for benzene (Figure 3.7 and Table 3.3). The regeneration of catalyst poses another problem as to how frequently the catalyst should be regenerated and what value of k should be used for designing the reactor. For a thirteen hour operation and regeneration cycle, the average k value (for all VOCs) ranges from $0.80 \text{ min}^{-1} \text{ m}^{-2}$ to $0.95 \text{ min}^{-1} \text{ m}^{-2}$ for 8W UV and $1.00 \text{ min}^{-1} \text{ m}^{-2}$ to $1.66 \text{ min}^{-1} \text{ m}^{-2}$ for 16W UV lamps. It is proposed that for 8W UV lamps the k value should be taken as $0.87 \text{ min}^{-1} \text{ m}^{-2}$ (average of the range of k value) and for 16W UV lamps it should be $1.3 \text{ min}^{-1} \text{ m}^{-2}$. This discussion also implies that reactor should be regenerated after every 12 hours of operation.

Three methods of catalyst regeneration were examined. Although all three methods (heating at 450 °C, washing with H₂O₂ and irradiation by UV lamp) can regenerate the catalyst in the range 98-92 percent of original k- value, it is recommended that the heating of reactor is the fastest and most efficient regeneration technique and should be followed. It may be stated that in the long-term laboratory experiments over two years, the same reactors have been regenerated over 100 times (by heating at 450°C). The regenerated catalyst can be used for a reasonable time; however, one should examine the catalyst performance for degradation of VOCs and its mechanical strength for long-term uses.

In summary, challenges and impediments of PCO technology using TiO₂ nano particles for VOC removal have been discussed and addressed for field application. The major issues of technology and remedial measures are (i) proper coating (including nano size particles) (ii) the wattage of UV lamp has positive impact on VOCs removal, a 16W UV lamp on average resulted in 25-30 percent higher degradation rate than a 8W UV lamp (iii) the catalyst should be regenerated after every 12 hours of operation to prevent substantial deactivation of surface and to account for progressive deactivation of surface and the average k value should be used for the design of reactor (e.g. 0.87 min⁻¹ m⁻² for 8W UV lamp and 1.3 min⁻¹ m⁻² for 16W UV lamp) rather than using the k value of freshly regenerated surface (Dhada et al., 2015b).

4 Field Application: Results and Discussion

The Chapter 3 has presented some impediments for application of PCO technology and these were duly addressed. It was concluded that the fabricated device with effective TiO₂ coating, usage of 16W UV light and regeneration of catalyst by heating were the best practices to enhance the performance of technology. In this chapter, effectiveness of developed device was demonstrated through three different case studies from the field: Case-1: Laboratory using benzene as solvent; Case-2: Conference room of a solvent industry using MCB, DCB and TCB; and Case 3: Chemistry laboratory using multiple VOCs (for details refer to Table 2.3). In all field applications, the catalyst surface was regenerated after every 12 hours of operation. Finally an on field pilot testing was done at the Aart Industries, Vapi.

4.1 Case-1: Laboratory Using Benzene as Solvent

The details of case study such as the size of the room, initial concentration of VOC, flow rate through the device and operation period of device are given in Table 2.3. The device (Figure 2.3) was first run without switching on the UV lights and it was observed that inlet and outlet concentrations of benzene were identical at the level of about 100 ppm. As soon as UV lights were switched on, within a few seconds, the benzene concentration at the outlet dropped to less than 1 ppm (Figure 4.1). The device was continuously operated for eight hours for varying inlet concentration of 76-160 ppm with an average removal efficiency of 99.54%. The device has performed exceptionally well for benzene removal..However, as stated earlier the formation of intermediates is of significant interest from health point-of-view. Formation of intermediates

(identification and quantification), their release to indoor environment and health risk from degradation of benzene are presented in Chapter 5, Risk characterization of exposure of intermediates

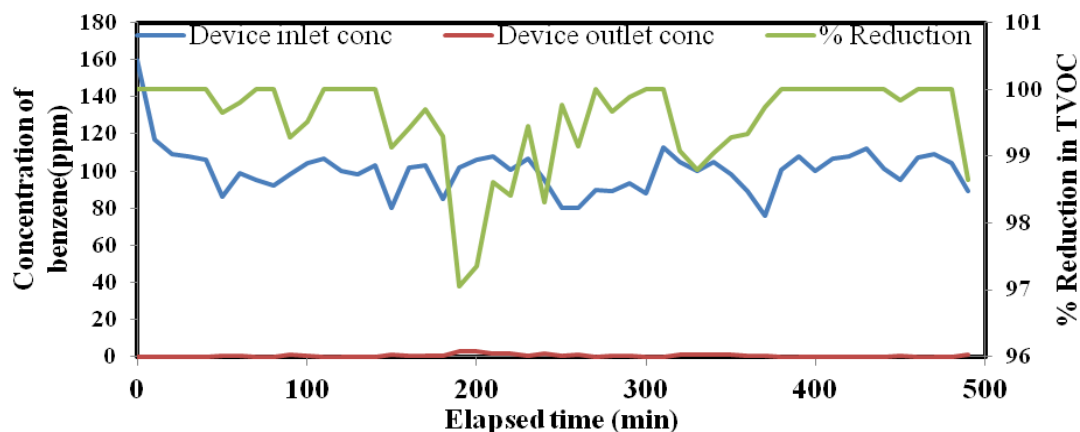


Figure 4.1: Performance of control device for degradation of benzene

4.2 Case-2: Conference Room of A Solvent Industry Using MCB, DCB and TCB

The details of this case study are given in Table 2.3. The device was installed in the conference room of an industry producing, storing and handling organic solvents (MCB, DCB and TCB) (Figure 4.2). Before discussing the performance of the device, the VOC concentration inside the room has been modelled by accounting for VOC infiltration of outdoor air, exfiltration of indoor air, VOC emission within the room and VOC removal achieved by the installed device.

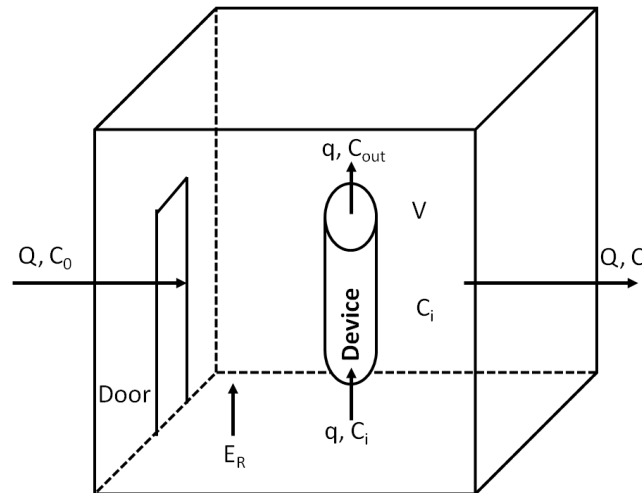


Figure 4.2: Schematic of conference room and installed VOC control system

Mass balance across the device: Adsorption of VOCs and the PCO on the catalyst surface can be represented by the Langmuir Hinshelwood equation (Kumar et al., 2008).

$$-\frac{dC}{dt} = \frac{k_d K_A C}{1 + K_A C} \quad (4.1)$$

Where, K_A is the adsorption coefficient for a gas on a material and k_d is the degradation rate constant (time^{-1}).

At low concentrations (ppm levels), the reaction reduces to a first order by neglecting the term $K_A C$ in the denominator ($1 \gg K_A C$).

$$-\frac{dC}{dt} = K_O C \quad (4.2)$$

Where, $K_O = k_d K_A$ (Overall degradation rate constant, time^{-1})

Assuming the device to be a plug flow reactor, at steady state, the outlet concentration can be expressed as

$$C_{\text{out}} = C_i e^{(-K_0 t_r)} \quad (4.3)$$

Where t_r is the retention time inside the device, C_{out} is the steady state VOC concentration at the outlet of the device and C_i is the steady state inlet concentration to the device which is same as the steady state concentration in the room.

Mass balance across the room: If room is considered as completely mixed, the VOC mass balance across the room (having the VOC control device) can be stated as:

$$\begin{aligned} \text{Accumulation} = & \text{rate of change in mass due to}[(\text{Infiltration of outdoor air}) \\ & + (\text{indoor generation}) - (\text{exfiltration of indoor air}) \\ & - (\text{removal through control device})] \end{aligned}$$

In mathematical terms

$$V \frac{dC_r}{dt} = QC_0 + E_R - QC_r - (C_r - C_{\text{out-d}})q \quad (4.4)$$

Where, C_0 : concentration of VOC entering in the room; Q : rate of flow of air in and out of the room; E_R : emission rate of VOC from a source in the room; V : volume of the room; q : rate of flow into the device, C_r is VOC concentration at any time inside the room and $C_{\text{out-d}}$ is VOC concentration at any time at the outlet of the device (refer to Figure 4.2 for the system and explanation of variables).

At steady state ($C_r = C_i$), the VOC concentration can be expressed as

$$C_i = \frac{QC_0 + E_R}{Q + q(1 - e^{-K_0 t_r})} \quad (4.5)$$

If N number of such devices installed (in parallel), C_i can be calculated as

$$C_i = \frac{QC_0 + E_R}{Q + Nq(1 - e^{-K_0 t_r})} \quad (4.6)$$

N that will be required to attain the desired steady state concentration, C_i can be calculated as:

$$N = \frac{Q(C_0 - C_i) + E_R}{qC_i(1 - e^{-K_0 t_r})} \quad (4.7)$$

Degradation rate constant per unit surface area of coating, $k = 1.79 \text{ min}^{-1} \text{ m}^{-2}$ is adopted from Dhada et al. (2015b), (Dhada et al., 2015b), $K_0 = 0.6104 \text{ min}^{-1}$ is obtained by multiplying k by TiO_2 coated surface area of seven reactors installed in the device ($A_r = 341 \times 10^{-3} \text{ m}^2$); rate of flow into the device $q = 4 \times 10^{-3} \text{ m}^3 \text{ min}^{-1}$ (at room condition); and measured concentration immediately outside the room $C_0 = 76 \text{ ppm}$, which enters the room through door with a flow rate of Q . The Q is estimated from the size of the door ($1 \text{ m} \times 2.1 \text{ m}$) and time required (2.3 seconds) to complete the cycle of door opening and closing. The measured average velocity of air at the time of door opening was $v = 1 \times 10^{-2} \text{ m sec}^{-1}$ (measured using anemometer: Lutron Anemometer; AM-4201). On average the door is opened 15 times during ten hours of working. Thus, rate of flow of air in and out of the room, $Q = 6.04 \times 10^{-3} \text{ m}^3 \text{ min}^{-1}$.

Figure 4.3 shows the performance of the control device in terms of its inlet and outlet TVOC concentrations. It is seen that a steady state concentration is attained in about 30 minutes both at inlet and outlet of the device. Initial TVOC concentration at $t=0$, was $76.0 \pm 6.0 \text{ ppm}$. The measured steady state concentration at the inlet of device was $63.0 \pm 5.0 \text{ ppm}$. It may be

noted that the steady state concentration at the inlet of the device is same as the steady state concentration in the room.

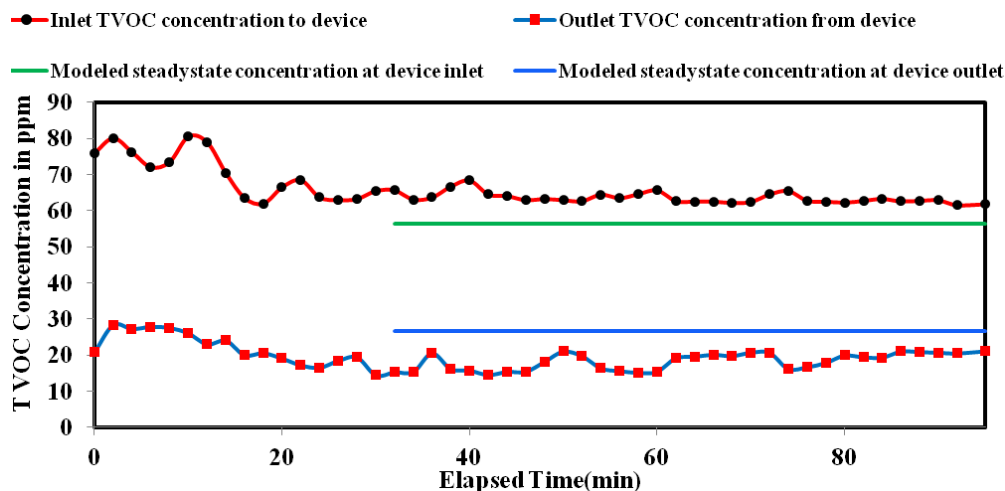


Figure 4.3: Modelled and observed TVOC concentrations at the device

By employing the developed model (Equation 4.6), the steady state concentration C_i in the room was calculated as 56.3 ppm. It suggests that model is performing well as measured and modelled concentrations (inside the room) are in close association (Figure 4.3). The measured steady state concentration at the outlet of device was 18.2 ± 3.6 ppm and the modelled steady state concentration (Equation 4.5) was 26.7 ppm (Figure 4.3). The model is over predicting concentration by 47 percent. The possible reason for such a discrepancy is that some of the VOCs may have adsorbed in the reactor, tubings, and teflon caps which were not accounted in the model formulation. The efficiency of the device at steady state was 71 percent. However, the effective VOC reduction attained in the room was only about 20 percent for one such device. It implies that we may have to install more such devices depending on the initial concentration in the room and finally desired VOC concentration.

Equation 4.7 can be used to estimate number of control devices required for obtaining the desired concentration of VOCs for the given size of the room, inlet VOC concentration to the room, emission rate inside the room and ventilation or airflow in the room. For the current case, Figure 4.4 shows the ratio of steady state concentrations (C_i/C_0) as a function of number of devices. Number of devices those may be required to bring the initial concentration of 76 ppm (considering TVOC is benzene) to ceiling limit of 25 ppm, set by occupational safety and health administration (OSHA) has been estimated as six (Figure 4.4).

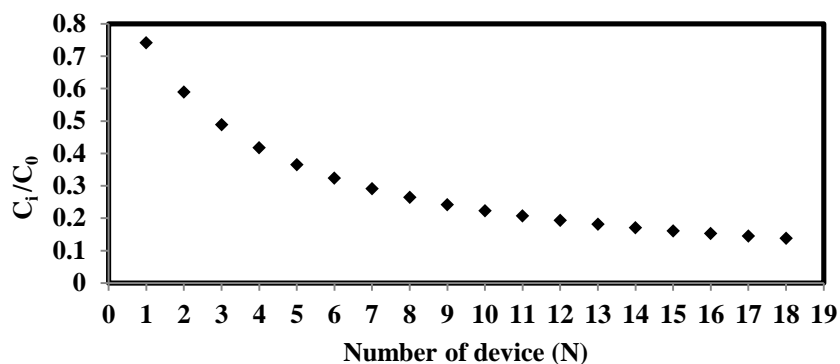


Figure 4.4: Ratio of steady state TVOC concentration inside the room and entering the room versus number of devices for Case-2

Although VOCs containing chlorine (MCB, DCB, TCB) have shown appreciable reduction (about 70%), formation of their intermediates and associated risk has not been assessed. There is a need to estimate the intermediates of VOCs containing halogens, other elements and metallic substituents and assess the risk of intermediates before technology is adopted for these VOCs.

4.3 Case-3: laboratory Using Multiple VOCs (Dichloromethane, Methanol, Ethyl acetate, Acetone, Hexane)

The details of case-3 - are presented in Table 2.3. The performance of device was evaluated at laboratory which was using multiple solvents/VOCs (dichloromethane, methanol, ethyl acetate, acetone and hexane). The retention time of TVOC in the device was calculated as 0.7 minutes. Figure 4.5 shows the performance of the control device in terms of inlet and outlet TVOC concentrations. It is seen that a steady state concentration is attained in about 100 minutes both at inlet and outlet of the device. The measured steady state concentration at the inlet of device was 73.0 ± 5.0 ppm (i.e. after 100 minutes). The measured steady state concentration at the outlet of device was 8.8 ± 3.0 ppm. The reduction efficiency of the device at steady state is 88.89%. The degradation rate constant, k for coexisting multiple VOCs was estimated at $1.06 \text{ min}^{-1} \text{ m}^{-2}$, which in comparison to k value of benzene ($1.6 \text{ min}^{-1} \text{ m}^{-2}$) (Dhada et al., 2015b) is 34 percent less. The degradation of multiple VOCs is expected to be slower than that of single compound. For multiple VOCs, the process is complex because of competitive reactions and formation of complex intermediate products of degradation which can deactivate the catalyst and impede the overall degradation (Dhada et al., 2015a).

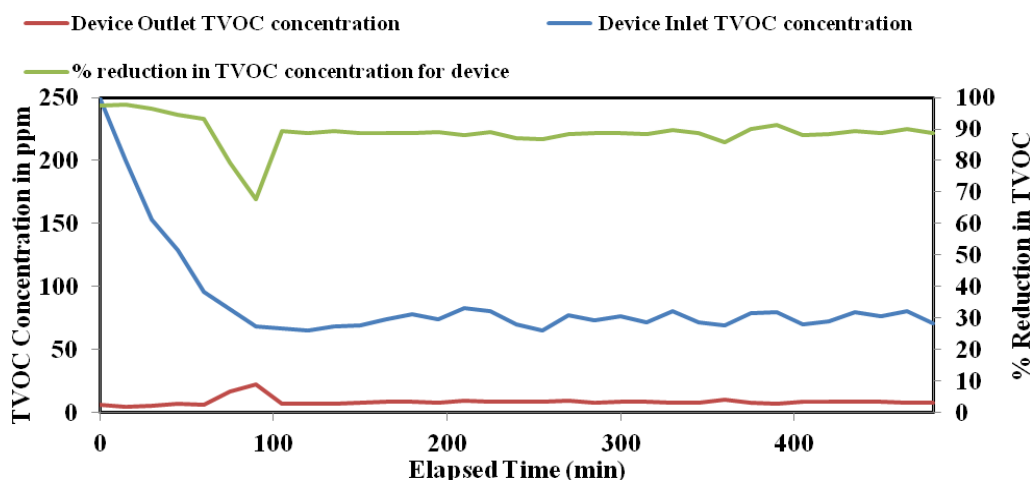


Figure 4.5: Performance of control device for degradation of TVOC in chemistry laboratory

The three case studies have taken the PCO technology to field and demonstrated its usefulness for the control of benzene, coexisting multiple VOCs and chlorobenzenes. The estimated degradation rate constant for coexisting multiple VOCs was $1.06 \text{ min}^{-1} \text{ m}^{-2}$ (surface area of catalyst), which in comparison to that of benzene ($1.6 \text{ min}^{-1} \text{ m}^{-2}$), is smaller by 34 percent. Possible reason for reduction in rate constant for multiple VOCs is occurrence of several concurrent competitive reactions on the surface of catalyst. The control efficiency of device was over 99 percent for benzene, 88 percent for multiple VOCs and 71 percent for chlorobenzenes.

4.4 Pilot Testing

4.4.1 Second Pilot Testing (July 17-22, 2014)

The VOC leakage points were monitored through a TVOC analyzer. The major leakages, outdoor sites (S1 to S5) with high concentrations were selected (Figure 4.6) for testing the VOC control device.

Outdoor sites

S1-Benzene feeding pump connected to vessel V101

S2-Feeding connected to drum tank (not in operation at the time of sampling)

S3-Near to the manometer of benzene tank V101

S4-Behand benzene tank V102

S5-Near to Column C-107



Initial assessment of VOCs leakage at Site 1



Initial assessment of VOCs leakages at Site 3



VOC Collection arrangement at Site1



Pilot Testing at Site-1

Figure 4.6: Testing the VOC control device

4.4.2 Performance of VOC Control System

(a) Site-1: Feed Pump

The system of VOC control system has performed satisfactorily with average removal efficiency of 61 percent and maximum efficiency of 91 percent (Table 4.1 and Figure 4.7).

Table 4.1: VOC Emission and Control at Site-1

Pump in operation			
Time	Inlet concentration (ppm)	Outlet concentration (ppm)	% Reduction
11:40	620	171	72.4
11:45	508	217	57.3
11:50	615	56	90.9
11:55	580	100	82.8
Average	581	136	75.8
Maximum	620	217	90.9
Minimum	508	56	57.3
Pump not in operation			
Time	Inlet concentration	Out let concentration	% Reduction
15:00	58.2	30.92	46.9
15:10	80	40.5	49.4
15:20	38.5	17	55.8
15:30	78	22.5	71.2
15:40	41	12	70.7
15:50	57	25	56.1
16:00	70.8	19.5	72.5
16:10	78.5	26	66.9
16:15	65	24.2	62.8
Average	63.0	24.2	61.4
Maximum	80.0	40.5	72.5
Minimum	38.5	12.0	46.9
StdDev	15.7	8.2	9.7

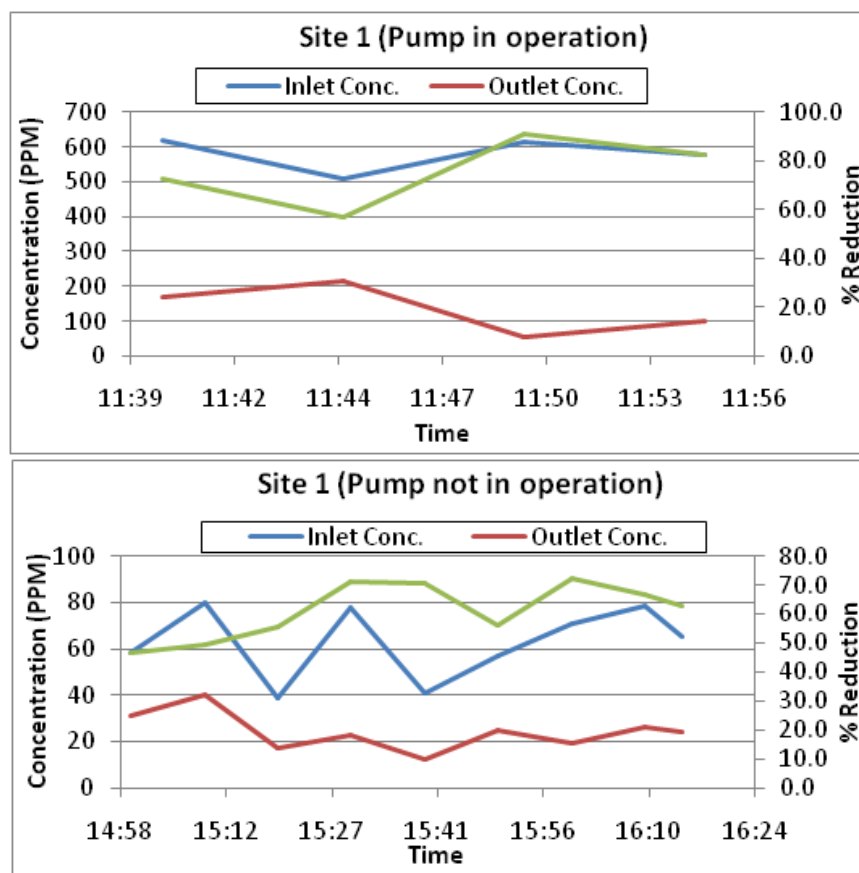


Figure 4.7: VOC Emission and Control at Site-1

(b) Site-2: Crude Feed Pump (20.7.2014)

The system of VOC control system has performed satisfactorily with average removal efficiency of 77 percent and maximum efficiency of 92 percent (Table 4.2 and Figure 4.8).

Table 4.2: VOC Emission and Control at Site-2 (Pump in operation)

Time	Inlet concentration	Out let concentration	% Reduction
14:05	650	125	80.8
14:08	750	63.4	91.5
14:11	1010	84	91.7
14:14	1600	470	70.6

14:17	1600	270	83.1
14:20	1660	373	77.5
14:23	922	291	68.4
14:26	3500	480	86.3
14:29	425	98	76.9
14:32	620	260	58.1
14:35	1400	445	68.2
14:38	1450	510	64.8
14:40	1800	327	81.8
Average	1337	292	76.9
Maximum	3500	510	91.7
Minimum	425	63	58.1
StdDev	796	160	10.4

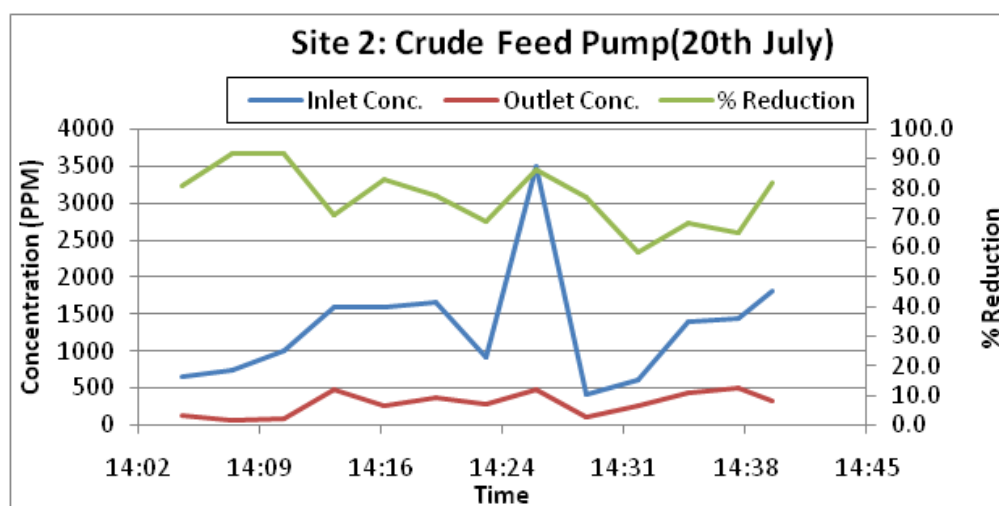


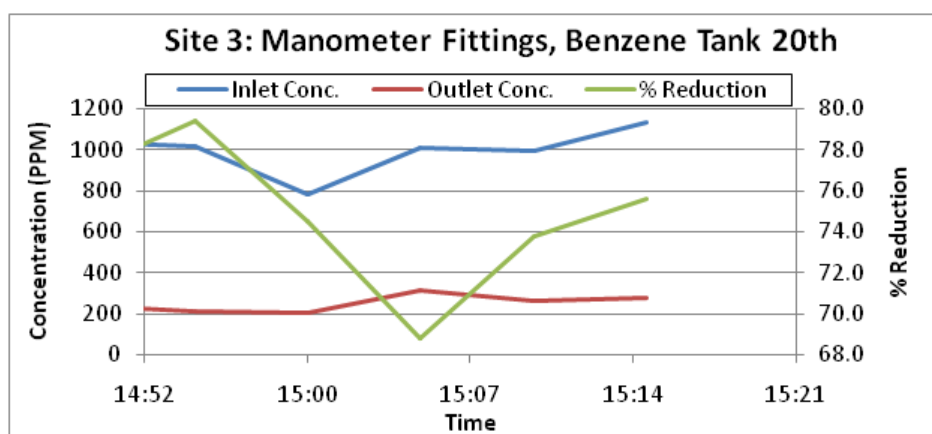
Figure 4.8: VOC Emission and Control at Site-2

(c) Site-3: Manometer Fittings, Benzene Tank

The system of VOC control system has performed satisfactorily with average removal efficiency of 75 percent and maximum efficiency of 80 percent (Table 4.3 and Figure 4.9).

Table 4.3: VOC Emission and Control at Site-3

Time	Inlet concentration	Out let concentration	% Reduction
14:50	1040	240	76.9
14:55	1020	210	79.4
15:00	785	200	74.5
15:05	1008	315	68.8
15:10	992	260	73.8
15:15	1132	276	75.6
Average	996	250	74.8
Maximum	1132	315	79.4
Minimum	785	200	68.8
StdDev	115	43	3.6

**Figure 4.9: VOC Emission and Control at Site-3**

The long-term performance of the site-3 is given below on a continuous basis (Table 4.4 and Figure 4.10); average VOC reduction is 92 percent.

Table 4.4: VOC Emission and Control at Site-3

Time	Inlet concentration	Out let concentration	% Reduction
15:35	136	13.23	90.3
15:38	225	6.04	97.3

Time	Inlet concentration	Out let concentration	% Reduction
15:41	350	12.4	96.5
15:44	198	15.31	92.3
15:47	130	14.02	89.2
15:50	350	12.97	96.3
15:53	183	12.68	93.1
15:56	308	16.18	94.7
15:59	167	19.14	88.5
16:02	193	25.16	87.0
16:05	149	19.8	86.7
16:08	187	23.2	87.6
16:11	240	19.3	92.0
16:14	130	18.76	85.6
16:17	250	16.42	93.4
16:20	193	12.6	93.5
16:23	94	11.01	88.3
16:26	215	9.3	95.7
16:29	168	12.07	92.8
16:32	294	12.51	95.7
16:35	153	12.5	91.8
16:38	297	13.3	95.5
16:41	257	9.47	96.3
16:44	143	9.73	93.2
16:47	240	9.63	96.0
16:50	520	16.03	96.9
16:53	114	14.02	87.7
16:56	217	15.1	93.0
16:59	113	13.28	88.2
17:02	116	9.4	91.9
17:05	151	12.52	91.7
17:08	138	11.01	92.0
17:11	167	15	91.0
17:14	145	14	90.3
17:17	206	14.38	93.0
17:20	151	16	89.4
17:23	119	17.08	85.6
17:26	167	13.42	92.0
17:29	357	24.31	93.2
17:32	198	14.37	92.7

Time	Inlet concentration	Out let concentration	% Reduction
17:35	137	15.87	88.4
17:38	269	16.11	94.0
17:41	279	28	90.0
17:44	248	20.94	91.6
17:47	250	16.2	93.5
17:50	143	9.13	93.6
17:53	205	13.15	93.6
17:56	217	18.51	91.5
18:00	314	24.1	92.3
Average	208	15.1	92.0
Maximum	520	28.0	97.3
Minimum	94	6.0	85.6
StdDev	82	4.6	3.1

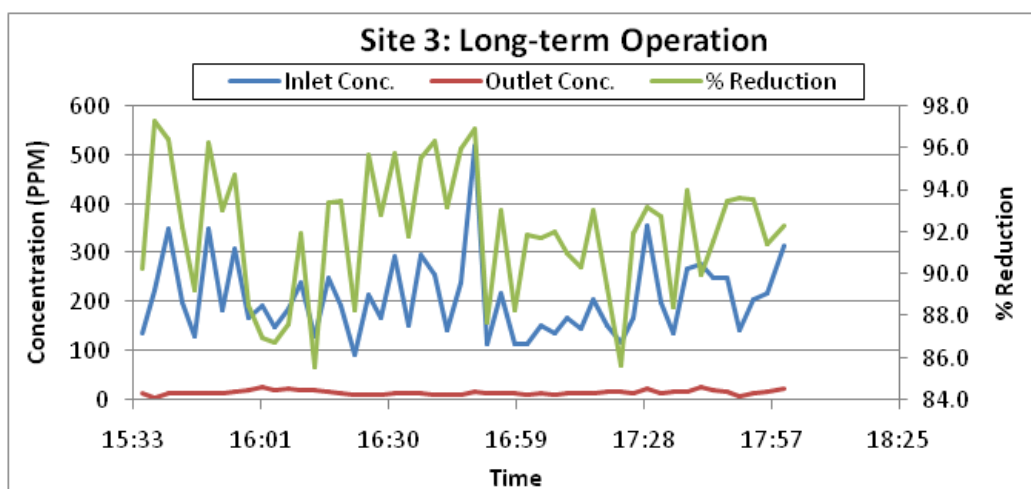


Figure 4.10: Long-term VOC Emission and Control at Site-3

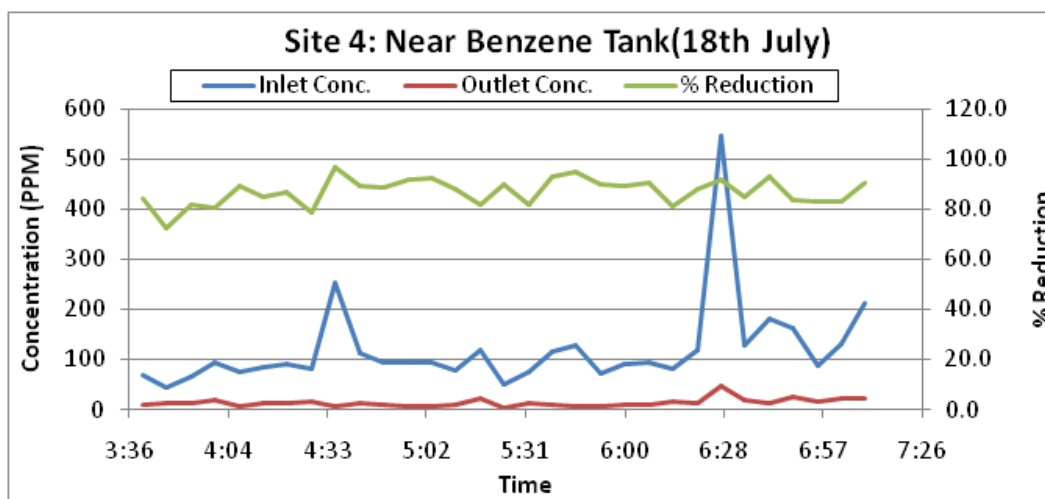
(d) Site-4

The performance at site-4 is shown below in Table 4.5 and Figure 4.11; average VOC reduction is 87 percent (18/07/2014) and 80 percent (19/07/2014).

Table 4.5: VOC Emission and Control at Site-4 on 18/07/2014 and 19/07/2014

18/07/2014			
Time	Inlet concentration	Out let Concentration	% Reduction
3:40	70	11.12	84.1
3:47	45	12.5	72.2
3:54	65	12	81.5
4:01	93	18	80.6
4:08	75	7.9	89.5
4:15	86	13	84.9
4:22	90	11.83	86.9
4:29	80	17	78.8
4:36	253	7.92	96.9
4:43	113	12	89.4
4:50	94	10.77	88.5
4:57	93	7.8	91.6
5:04	95	7.3	92.3
5:11	79	9.6	87.8
5:18	120	22	81.7
5:25	49	4.97	89.9
5:32	75	13.5	82.0
5:39	115	8.2	92.9
5:46	127	6.37	95.0
5:53	71	7.2	89.9
6:00	91	9.9	89.1
6:07	93	8.64	90.7
6:14	81	15.2	81.2
6:21	120	14.21	88.2
6:28	546	46	91.6
6:35	128	19	85.2
6:42	182	12.9	92.9
6:49	162	26.35	83.7
6:56	88	14.96	83.0
7:03	132	22.14	83.2
7:10	211	20.65	90.2
Average	120	13.9	86.9
Maximum	546	46.0	96.9
Minimum	45	5.0	72.2
StdDev	91	7.9	5.4

19/07/2014			
Time	Inlet concentration	Out let concentration	% Reduction
12:00	180.12	23.6	86.9
12:10	85.32	15.6	81.7
12:20	152.12	38.16	74.9
12:30	109	12	89.0
12:40	92	8.5	90.8
12:50	244	46	81.1
13:00	125.3	21.4	82.9
13:10	150	30	80.0
13:20	125	33	73.6
13:30	110	25	77.3
13:40	250	51.2	79.5
13:50	24	5	79.2
14:00	58	15	74.1
14:10	87	30	65.5
14:15	124	31	75.0
14:20	260	83	68.1
14:25	250	2.01	99.2
14:30	78	10	87.2
Average	139	26.7	80.3
Maximum	260	83.0	99.2
Minimum	24	2.0	65.5
StdDev	71	19.6	8.3



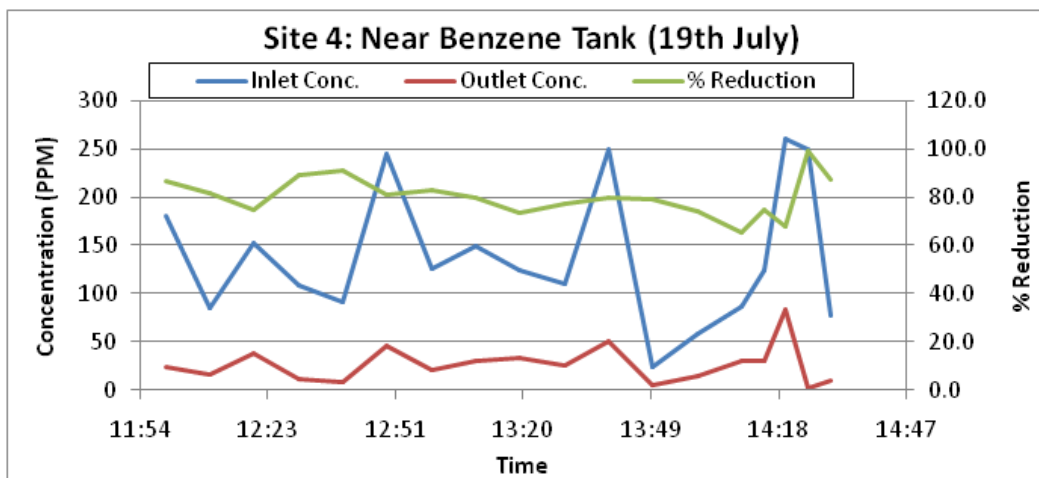


Figure 4.11: VOC Emission and Control at Site-4 on 18th and 19th July 2014

(e) Site-5

Figure 4.12 shows the features at site-5. The performance at site 5 is shown below in Table 4.6 and Figure 4.13; average VOC reduction is 70 percent.



Operation of mini-pilot plant for Monitoring VOC at Site-5



Inlet concentration at Site 5



Outlet concentration at Site 5

Figure 4.12: Testing of mini-pilot plant at site-5

Table 4.6: VOC Emission and Control at Site-5

Time	Inlet concentration	Out let concentration	% Reduction
12:25	1500	140	90.7
12:28	46	21	54.3
12:31	230	25	89.1
12:34	141	27	80.9
12:37	51	13	74.5
12:40	38	13	65.8
12:43	180	17	90.6
12:46	27	10	63.0
12:49	692	54	92.2
12:52	223	45	79.8
12:55	113	28	75.2
12:58	583	50	91.4
13:01	638	69	89.2
13:04	110	41	62.7
13:07	209	29	86.1
13:10	650	150	76.9
13:13	340	80	76.5
13:16	587	257	56.2
13:19	356	190	46.6
13:22	452	82	81.9
13:25	792	206	74.0
13:28	761	188	75.3
13:31	80	53	33.8
13:34	649	227	65.0
13:37	730	229	68.6
13:40	232	143	38.4
13:43	730	132	81.9
13:46	94	61	35.1
13:49	981	316	67.8
13:52	757	58	92.3
13:55	761	100	86.9
13:58	97	26	73.2
14:01	86	25	70.9
14:04	67	21	68.7
14:07	664	110	83.4
14:10	744	120	83.9
14:13	527	96	81.8

Time	Inlet concentration	Out let concentration	% Reduction
14:16	749	241	67.8
14:19	991	236	76.2
14:22	553	232	58.0
14:25	388	71	81.7
14:28	784	198	74.7
14:31	1056	350	66.9
14:34	891	260	70.8
14:37	780	208	73.3
14:40	516	216	58.1
14:43	450	162	64.0
14:46	390	166	57.4
14:49	600	272	54.7
14:52	480	234	51.3
14:55	397	194	51.1
14:58	315	114	63.8
15:01	74	35	52.7
15:04	89	42	52.8
15:07	190	39	79.5
Average	466	122	70.2
Maximum	1500	350	92.3
Minimum	27	10	33.8
StdDev	328	92	14.8

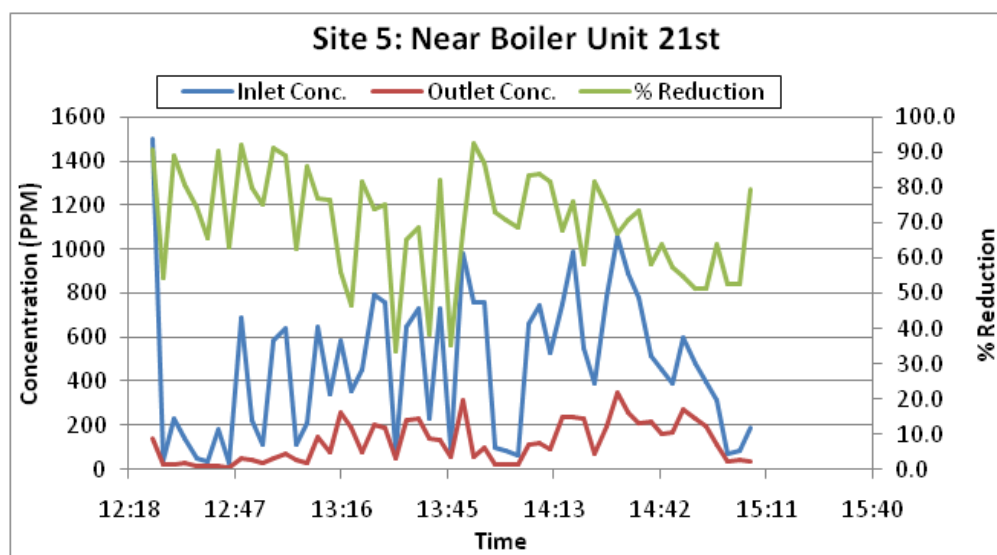


Figure 4.13: VOC Emission and Control at Site-5

4.4.3 *Interpretation of Results of pilot Testing and Way forward*

- The pilot plant for VOC control has performed very well with an average VOC control at multiple sites has been over 75 percent with maximum removal of over 92 percent. This pilot testing establishes the technology, especially under varying inlet VOC concentration 2000 ppm.
- One of the major constraints in adopting the technology is that the inlet concentration is significantly varying at the plant. While the average concentration is around 500-600 ppm, the peak concentration may go well above 2000 ppm. Such a surge of concentration can quickly deposit on the surface by condensation and deactivate the catalyst and thus the efficiency can reduce dramatically and the catalyst surface needs to be regenerated. It is important that the control device be revamped in terms of dilution chamber for uniform inlet VOC concentration to the control device.
- Industry expects that control setup should be easy to operate and maintain.
- While monitoring, it was felt that air sucked in to the system must be particulate free and should not have very fast fluctuation. A surge tank/tube filled/fitted with Teflon filter may be one solution to ensure stable operation of the prototype mini pilot plant (MPP). This needs to be done and tested.
- Research team feel that tube if fitted in MPP should be horizontal for an easy installation and dismantling of the tube after regeneration.
- Several sets of data reveal that system is suitable for variable field conditions. Quantitative data must be generated to support decision that when tubes need to be regenerated. Tubes should be self-indicated by colour when regeneration is required.

Total timer (TT) reading set for few reading and range of concentration to which system was been exposed can also be used to take decision on regeneration.

For technology/device to handle unusually high concentration, modifications are required in the device and again tested for the long –term performance. The testing could not be completed due to constant rains at the site till September 2014. The rainy also caused very high humidity which could condense at the active site and this problem had to be corrected. The above modifications have been done and the device requires validation on field before being used for long time.

4.5 The New Control Equipment

The new equipment was designed based on the degradation rates estimated from laboratory studies (carried out in this project) reduction in the efficacy of catalyst with its use. The impediment and difficulties encountered in earlier versions have been taken in consideration while designing the new units. The specific features of the new equipment are given below. The pictures inside and outside of the devices are given below.

- The device can handle about 90 litres per minute (LPM) of polluted air compared to earlier system handling 6-10 LPM of air
- The device is made of aluminium which is light in weight which is easy transport
- The coating substrate is aluminium plates and not glass which was fragile and could break
- The system uses both sides of the plates for catalyst coating and thus will have improved VOC reduction

- The coated plates are of front loading and thus has an ease of operation (while inserting or taking out the plates)
- All the connections through narrow tubes and holes have been avoided and thus pressure drop is minimized.
- The temperature and humidity meters have been installed for better control of process
- The overall dimension is 140 cm× 35 cm× 30 cm with eight number of plates (30 cm × 20 cm)
- There are total 24 UV lights of 16 W each capacity
- The system is completely enclosed to avoid the exposure to the UV light
- Special feature is the design of see through glass window for assessing operation of the system.
- An air tight and leak-proof system.

The new equipment was tested and it showed an average reduction of about 75% in benzene.





Figure 4.14: Images of the New VOC Control System

5 Risk Characterization of Exposure to Intermediates

In Chapter 4, effectiveness of the developed device was evaluated through three different case studies (for details refer to Table 2.3) and on newly designed system. The complete oxidation of VOCs does not happen instantly. Some intermediates are formed due to partial oxidation and can get released in the surrounding air which may be harmful to the building occupants. Harmful intermediates could be a major impediment for field application of PCO technology. In addition to vapour phase intermediates, some partially oxidised semi-volatiles (referred to as solid phase intermediates) can deposit on the catalyst surface and may be released when catalyst is regenerated. This chapter presents quantification of intermediates of PCO of benzene (Case-1: Table 2.3) and that for PCO of EXT. The exposure risk of intermediates has been assessed for BTEX.

5.1 Solid Phase Intermediates of Benzene

For Case-1 of PCO of benzene (Table 2.3), the intermediates adsorbed on the surface of the catalyst were extracted and analysed (see section 2.2.1). During regeneration of the catalyst, these intermediates are released and may pose risk to the occupants of the building. GC-MS was used to identify the intermediates and these include: (a) those reported in the literature and identified: phenol, methyl-cyclo-pentane, pentane, acetone, hexane, cyclo-hexane, 1,4-benzoquinone, benzaldehyde, benzyl alcohol, cresol, hydroquinone, benzoic acid, benzene (Jacoby et al., 1996; Cao et al., 2000; Guo et al., 2008; Han et al., 2008; Mo et al., 2009a; Sleiman et al., 2009); and (b) those identified solely in this study: 4-methyl-phenol-(4-cresol),

methyl-cyclo-hexane, 2,2,4-tri-methyl hexane and 2,2,3-tri-methyl-decane etc. (See Table S1; Appendix A). Some of the intermediates (acetone, benzoic acid, hexane and phenol etc) for which standards were available have been quantified. Figure 5.1 shows mass in μg of intermediate per mg of benzene removed per sq-metre surface area of the catalyst in 8 hour of operation of device. The major intermediates which may affect the photocatalytic activity of TiO_2 surface are acetone and benzoic acid. The intermediates (about 4.44 percent of benzene mass removed) are released during catalyst regeneration. The health risk assessment of these intermediates is discussed in section 5.3.

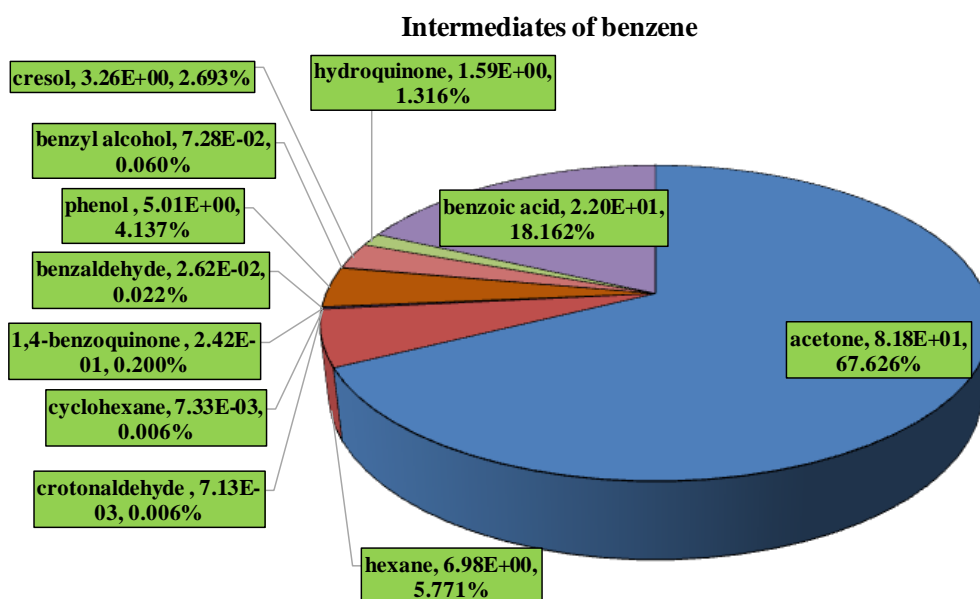


Figure 5.1: Mass of intermediates (μg) adsorbed on the catalyst for each mg of benzene removed per sq-metre surface area of catalyst coating (8 hour operation)

5.2 Intermediates of EXT

5.2.1 Vapour Phase

The EXT (initial concentration: 180 mg/m³; 190 mg/m³; 130 mg/m³, 170 mg/m³; as per Table 2.4, column 2) was introduced in the batch reactor for identification and quantification of intermediates. The initial concentrations were high compared to the levels observed in indoor air (Table 2.4; column 3) so that measurable amounts of intermediates are obtained. The concentration of the intermediates will depend on the surface area of the catalyst coating and amount of parent VOC removed. The intermediates in vapour phase were sampled and analysed as per the method described in section 2.3.1.

Table 5.1 presents mass of vapour phase intermediates produced per mg of ethylbenzene removed per sq-metre surface area of catalyst (for operating period of 40, 80, 120, 160 and 200 minutes). For a realistic continuous operation of the reactor for 12 hours, it was assumed that after 200 minutes, there was no reduction in mass of intermediates and at every 40 minute, same initial mass of ethylbenzene (i.e. 142.40 mg) enters the reactor for treatment; this is done to mimic the continuous operation of the reactor. As an example, calculation of mass of toluene (one of the intermediates) released in 12 hour is shown here (each term shows the amount released in every 40 minutes for 12 hours of operation): [11.23 + (11.23+20.1) + (11.23+20.1+11.17).....till 18th term]/18=103.34 µg per mg of ethylbenzene removed per sq-meter of surface area of catalyst.

Table 5.1: Mass of intermediates produced from PCO of ethylbenzene

Time of operation (minutes)	Ethylbenzene (mg)	Measured mass of intermediates(μg) per mg of ethylbenzene removed per sq-meter surface area of catalyst coating					
		Hexane	Benzene	Toluene	Phenol	Benzoic acid	Hydroquinone
0	142.40	0.00	0.00	0.00	0.00	0.00	0.00
40	4.73	0.00	0.00	11.23	0.00	0.00	0.00
80	2.44	41.88	6.57	20.10	0.00	0.00	0.00
120	0.93	20.19	8.36	11.17	0.00	0.00	0.00
160	0.42	46.16	4.79	11.16	0.00	5.75	2.40
200	0.34	29.88	0.00	9.24	0.98	5.56	2.10
		Estimated total mass of intermediates produced (μg per mg of ethylbenzene removed per sq-meter surface area of catalyst coating)					
720	-	270.24	17.62	103.34	5.72	37.21	14.24

Similar to estimates of intermediates produced from PCO of ethylbenzene, the intermediates of PCO of xylene and toluene in the vapour phase for 12hour operation are presented in Table6.2. It can be seen that among the intermediates of ethylbenzene, hexane is the major intermediate followed by toluene and benzoic acid. Among the intermediates of p, m-xylene, benzoic acid is the major intermediate followed by hydroquinone and benzyl alcohol. Among the intermediates of o-xylene, hexane is the major intermediate followed by benzoic acid and hydroquinone. Among the intermediates of toluene, benzoic acid is the major intermediate followed by hydroquinone and benzene. Benzoic acid and hydroquinone are the common intermediates in PCO of EXT.

Table 5.2: Mass of intermediates produced from PCO of xylenes and toluene (Vapour phase)

Intermediates	Measured mass of intermediates(μg) per mg of VOCs removed per sq-meter surface area of catalyst coating (12hour continuous operation)		
	p, m- xylene	o-xylene	Toluene
Acetone	-	0.55	7.63
Hexane	-	202.24	8.21
Phenol	-	9.54	-
Benzoic acid	48.47	49.35	55.32
Hydroquinone	46.48	41.38	33.81
Pentane	5.83	-	-
Toluene	10.69	-	-
Benzyl alcohol	20.12	-	-
1,4 benzoquinone	4.53	-	-
Benzyldehyde	-	-	4.50

5.2.2 Solid Phase

The intermediates (of ethyl benzene, p,m,o-xylene, toluene) adsorbed on the surface of the reactors in continuous 12 hour operation and likely to be released on regenerating the catalyst are presented in Figures 5.2 - 5.5 and Table 5.3. The major intermediates of ethylbenzene are (Figure 5.2) benzoic acid followed by cresol, hexane and acetone and these account for 3.30% of mass of the ethylbenzene removed. The major intermediates of p,m-xylene, as shown in Figure 5.3, are hexane followed by benzoic acid, acetone and crotonaldehyde and these account for 2.27% of mass of the p,m-xylene removed. The major intermediates of o-xylene as shown in Figure 5.4 are acetone followed by hexane and benzoic acid and account for 4.14% of mass of the o-xylene removed. The major intermediates of toluene, as shown in Figure 5.5, are acetone followed by benzoic acid and hydroquinone and account for 2.96% of mass of the toluene removed.

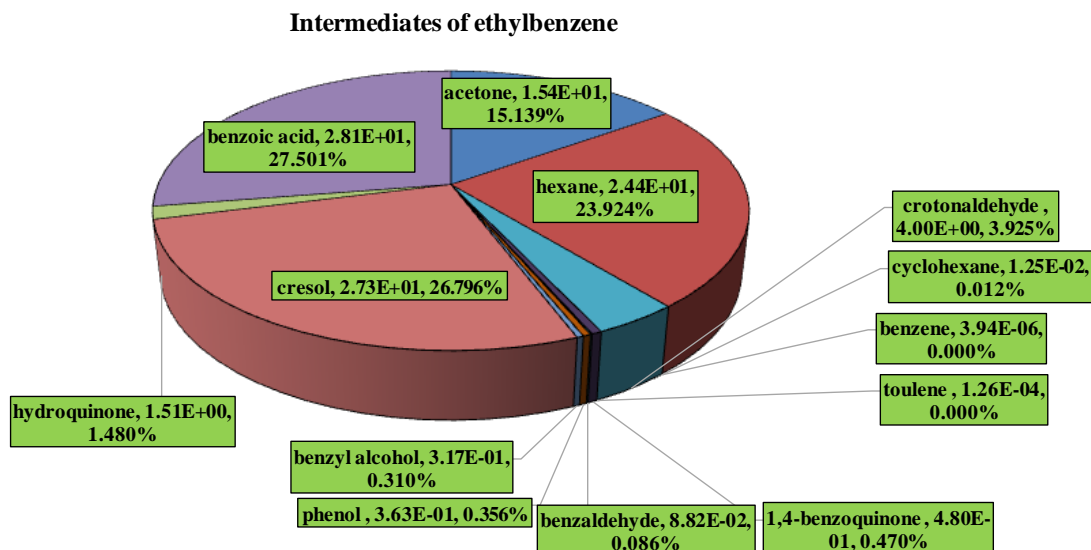


Figure 5.2: Mass of intermediates (μg) adsorbed on the catalyst for each mg of ethylbenzene removed per sq-meter surface area of catalyst coating

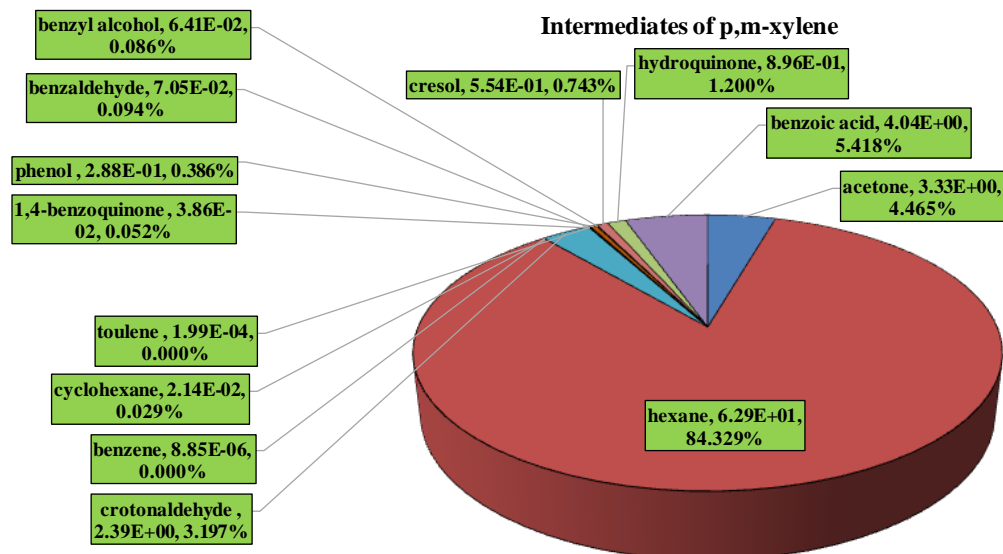


Figure 5.3: Mass of intermediates (μg) adsorbed on the catalyst for each mg of p,m-xylene removed per sq-meter surface area of catalyst coating

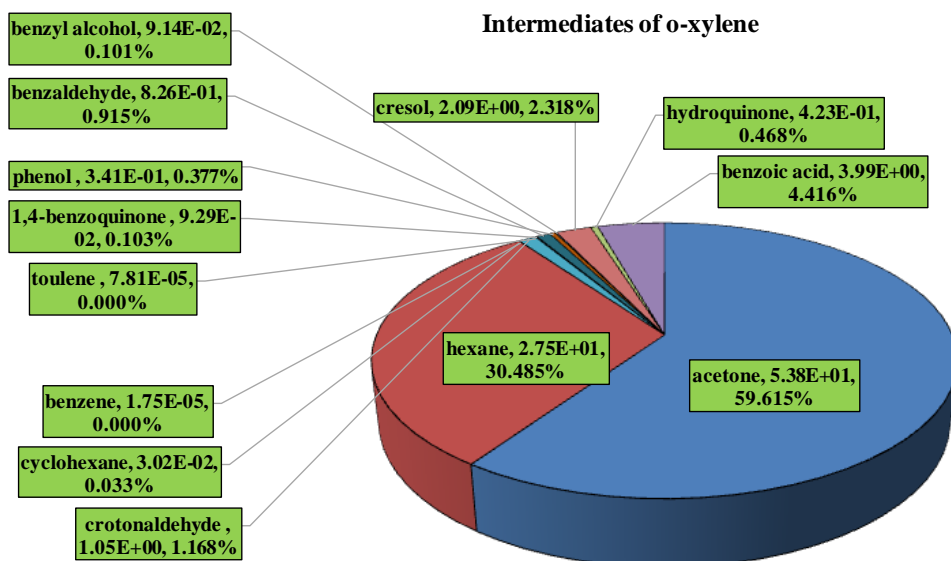


Figure 5.4: Mass of intermediates (μg) adsorbed on the catalyst for each mg of o-xylene removed per sq-meter surface area of catalyst coating

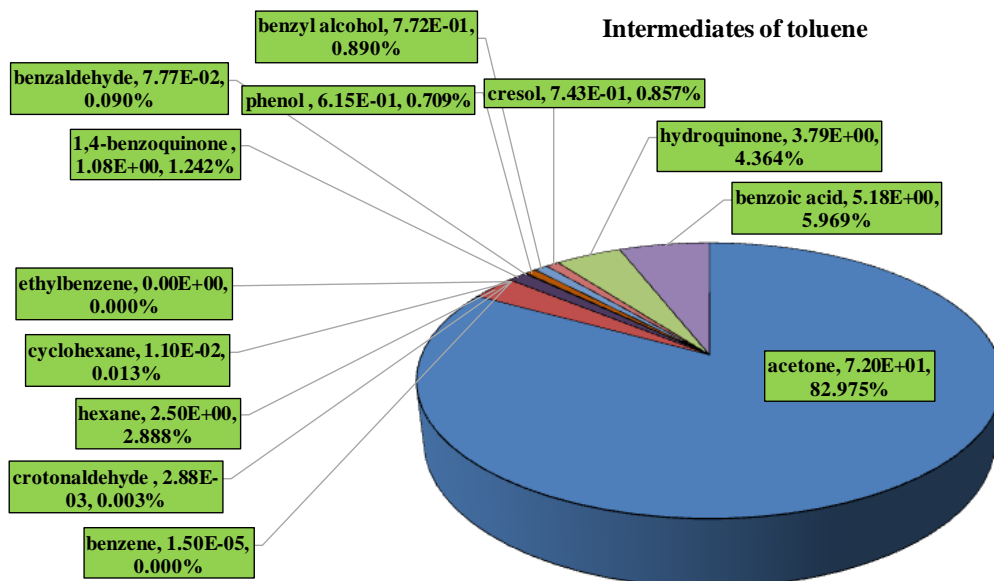


Figure 5.5: Mass of intermediates (μg) adsorbed on the catalyst for each mg of toluene removed per sq-meter surface area of catalyst coating

Table 5.3: Mass of intermediates released from PCO of EXT (μg per mg of EXT removed per sq-meter surface area of catalyst coating in 12hour continuous operation; solid phase)

Intermediates	VOCs			
	Ethylbenzene	p,m- xylene	o- xylene	Toluene
Acetone	1.55E+01	3.33E+00	5.37E+01	7.20E+01
Hexane	2.44E+01	6.30E+01	2.75E+01	2.51E+00
Cyclohexane	1.25E-02	2.14E-02	3.03E-02	1.10E-02
Benzene	3.93E-06	8.86E-06	1.75E-05	1.50E-05
Crotonaldehyde	4.01E+00	2.39E+00	1.06E+00	2.89E-03
Toulene	1.26E-04	1.98E-04	7.80E-05	3.93E-05
1,4-benzoquinone	4.80E-01	3.87E-02	9.30E-02	1.08E+00
Benzaldehyde	8.83E-02	7.06E-02	8.26E-01	7.77E-02
Phenol	3.63E-01	2.89E-01	3.41E-01	6.16E-01
Benzyl alcohol	3.16E-01	6.41E-02	9.13E-02	7.72E-01
Cresol	2.73E+01	5.53E-01	2.09E+00	7.44E-01
Hydroquinone	1.51E+00	8.97E-01	4.23E-01	3.79E+00
Benzoic acid	2.81E+01	4.03E+00	3.98E+00	5.18E+00

The probable intermediates of PCO of EXT with their retention time (RT) in GC-MS are presented in Appendix-A.

5.3 Risk Assessment of Intermediates

5.3.1 Risk Assessment of Exposure to Intermediates of Benzene

For the purposes of estimating the risk of solid phase intermediates of benzene, it is assumed that (i) concentration of benzene in the room is $220 \mu\text{g}/\text{m}^3$ (highest benzene concentration observed in indoor air: Sexton et al. (2004)), (ii) volume of the room is 195 m^3 and (iii) the device having seven reactors (size of one reactor: $7.0\text{E}-4\text{m}^3$) in series was operated for 12 hours. For intermediates of benzene, the estimated CA, HI and carcinogenic risk (defined in Section 2.3.2),

were presented in Table 5.4. It can be seen from the table that the cancerous risk is in the order of 10^{-9} and overall HI ($7.21E-05$) is well below the permissible limit of 1.0.

Table 5.4: Indoor air concentration of intermediates (solid phase) and health risk (Volume of room 195 m^3 and mass of benzene treated 1.108 mg in 12 hours of operation)

Intermediates	CA (mg/m ³)	CDI (mg/kg-day)	RfD (mg/kg-day)	Carcinogenic Risk(SF×CDI)	HI
Acetone	1.71E-04	5.79E-06	1.00E-01		5.79E-05
Hexane	1.46E-05	4.94E-07	5.72E-02		8.63E-06
Cyclohexane	1.53E-08	5.19E-10	1.71E-00 [#]		3.03E-10
Crotonaldehyde	1.49E-08	5.04E-10	-	9.58E-10*	
1,4-Benzoquinone [@]	5.05E-07	1.71E-08	-		
Benzaldehyde	5.46E-08	1.85E-09	1.00E-01 ^o		1.85E-08
Phenol	1.04E-05	3.54E-07	6.00E-01		5.90E-07
Benzyl alcohol	1.52E-07	5.15E-09	3.00E-01 ^o		1.72E-08
Cresol	6.79E-06	2.30E-07	5.00E-02		4.61E-06
Hydroquinone [@]	3.32E-06	1.13E-07	-		
Benzoic acid	4.58E-05	1.55E-06	4.00E+00		3.89E-07
			$\Sigma =$	9.58E-10	7.21E-05

* Slope factor for crotonaldehyde is $=1.9/\text{mg}/\text{kg}/\text{day}$ (GSI Environmental 2013),

[@] RfD is not available for 1,4 benzoquinone and hydroquinone,

[#] (U.S.E.P.A(US Environmental Protection Agency) 2003)

^o (GSI Environmental 2013)

5.3.2 Risk assessment of Exposure to Intermediates of EXT

For demonstrating the risk assessment, it is assumed that a device consisting of seven reactors in series treats the initial concentration of EXT (ethylbenzene: $220 \mu\text{g}/\text{m}^3$; p,m-xylene: $260 \mu\text{g}/\text{m}^3$; o-xylene: $260 \mu\text{g}/\text{m}^3$; toluene: $320.5 \mu\text{g}/\text{m}^3$) at a flow rate of 7 lpm for a laboratory of volume 195 m^3 . The estimated CA, HI and carcinogenic risk for ethylbenzene are given in Table 5.5. It can be seen from the Table that the cancerous risk is in the order of 10^{-6} and overall HI ($1.18E-03$) is well below the permissible limit of 1.0.

Table 5.5: Indoor air concentration of intermediates (vapour and solid phase) of PCO of ethylbenzene and health risk (Volume of room 195 m³ and mass of ethylbenzene treated 1.188 mg)

Intermediates	CA (mg/m ³)	CDI (mg/kg- day)	RfD (mg/kg- day)	Carcinogenic Risk(SF×CDI)	HI	
Vapour phase						
Hexane	5.64E-04	5.35E-05	3.82E-02		9.35E-04	
Benzene	3.68E-05	3.49E-06	1.90E-01*	1.01E-07		
Toluene	2.16E-04	2.04E-05	9.34E-01		1.46E-05	
Phenol	1.19E-05	1.13E-06	4.00E-01		1.88E-06	
Benzoic acid	7.76E-05	7.36E-06	2.67E+00		1.84E-06	
Hydroquinone	2.97E-05	2.82E-06	@			
				Σ=	1.01E-07	9.53E-04
Solid phase						
Acetone	3.22E-05	3.06E-06	1.00E-01		3.06E-05	
Hexane	5.09E-05	4.83E-06	5.72E-02		8.44E-05	
Cyclohexane	2.61E-08	2.48E-09	1.71E+00 [#]		1.45E-09	
Benzene	8.21E-12	7.79E-13	2.90E-01*	3.65E-14		
Crotonaldehyde	8.35E-06	7.92E-07	1.90E+00*	2.43E-06		
Toulene	2.62E-10	2.49E-11	1.40E+00		1.78E-11	
1,4- benzoquinone	1.00E-06	9.49E-08	@			
Benzaldehyde	1.84E-07	1.74E-08	1.00E-01 ^o		1.74E-07	
Phenol	7.57E-07	7.18E-08	6.00E-01		1.20E-07	
Benzyl alcohol	6.60E-07	6.26E-08	3.00E-01 ^o		2.09E-07	
Cresol	5.70E-05	5.41E-06	5.00E-02		1.08E-04	
Hydroquinone	3.15E-06	2.99E-07	@			
Benzoic acid	5.85E-05	5.55E-06	4.00E+00		1.39E-06	
				Σ =	1.51E-06	2.25E-04
Overall (vapourphase+solid phase) =					1.61E-06	1.18E-03

[@] RfD is not available for 1,4 benzoquinone and hydroquinone

[#] (U.S.E.P.A(US Environmental Protection Agency) 2003)

^o (GSI Environmental 2013)

* Slope factor, slope factor for crotonaldehyde is =1.9/mg/kg/day)(GSI Environmental 2013)

Likewise risk assessment of intermediates of ethylbenzene, the risk of intermediates of p,m-xylene (see Table S2, Apendix-B), o-xylene (see Table S3, Apendix-B) and toluene (see Table S4, Apendix-B) has been assessed. The overall risk of intermediates of BTEX is presented

in Figure 5.6 (Carcinogenic risk) and Figure 5.7 (Hazard index). It can be seen from the Table that the cancerous risk is in the order of 10^{-6} and overall HI is well below 1.0.

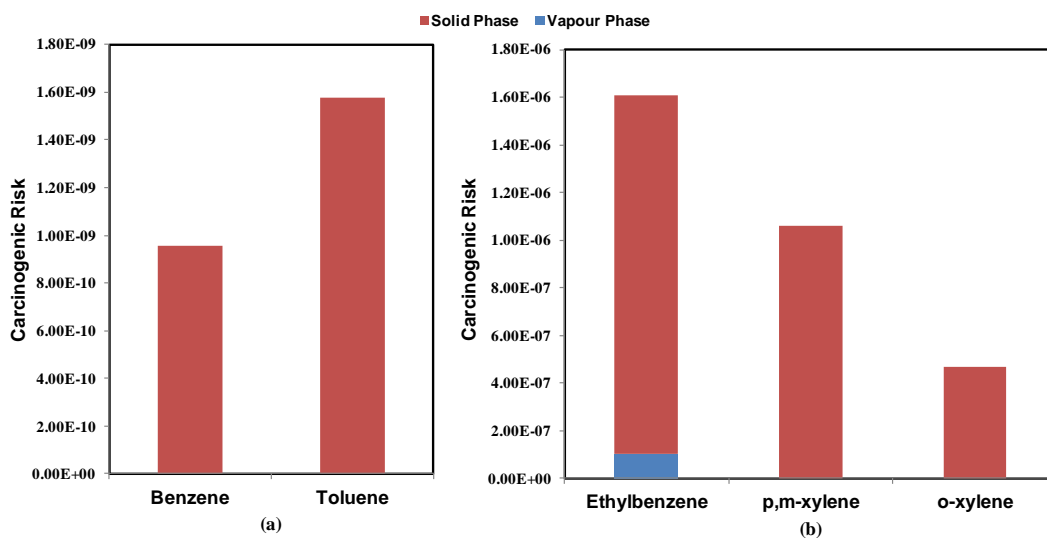


Figure 5.6: Carcinogenic risk for vapour and solid phase (except benzene) intermediates of BTEX

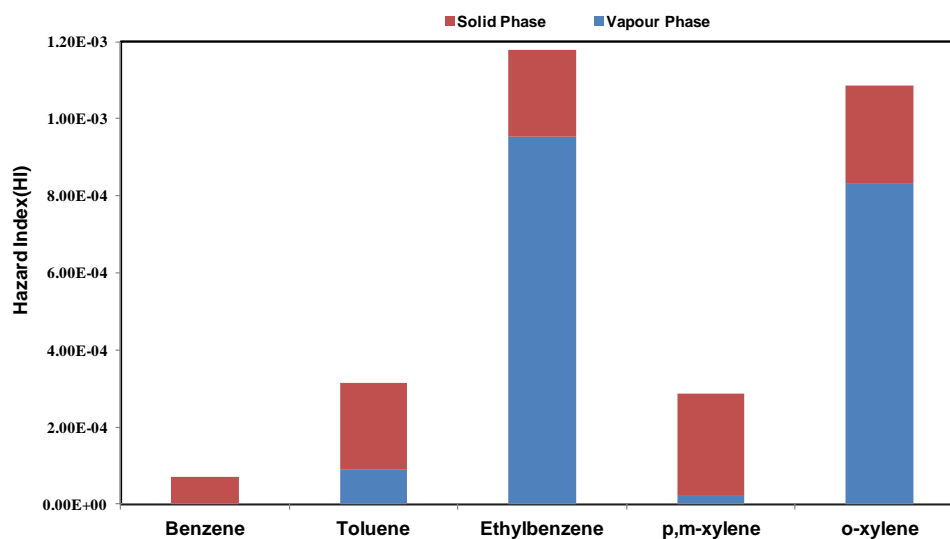


Figure 5.7: Hazard index for vapour and solid phase (except benzene) intermediates of BTEX

It is concluded that the risk associated with the intermediates of photo-degradation of BEXT is well within acceptable limits and the technology can be adopted with confidence. It is

to be noted that carcinogenic risk is higher from intermediates adsorbed on the catalyst surface (solid phase) than vapour phase intermediates. For HI, the risk is much higher (71-93%) from the solid phase intermediates of toluene and p,m-xylene. For o-xylene and ethylbenzene, HI is higher (77-80%) for vapour phase intermediates. The users of technology are well advised to release the vapour from catalyst regeneration process outside the room and away from the inlet of fresh air for air conditioning. This will ensure dilution of harmful intermediates.

In summary, this study has identified and quantified the intermediates of degradation of BTEX (both in vapour phase (except benzene) and those from catalyst regeneration), estimated the human health risk of exposure of intermediates for long-term laboratory occupants and suggested the pathways of degradation. There are new findings in suggesting the pathways of EX, which were not studied earlier. The carcinogenic risk and HI both are within level and technology can be adopted in field. Although the health risk is acceptable, it is suggested that the outlet of the control device and that of catalyst regeneration is kept outside the laboratory / room and intermediates are released in ambient air where better dispersion can be achieved.

6

Summary and Conclusions

6.1 Summary

TiO₂-based photocatalytic oxidation (PCO) of VOCs is well established in theory and at laboratory scale. However, the technology has not attracted many commercial and field applications. The challenges and impediments those have prevented the TiO₂-based PCO technology from becoming widely accepted have been identified, discussed and addressed in a scientific manner. Proper TiO₂ coating, UV intensity, humidity, temperature, particle size, phase of catalyst, degradation constant and regeneration of catalyst surface are of paramount significance for field application. For any catalytic process in which catalyst degrades with time, the challenge is in delineating catalyst efficacy that can be used in designing the process and how frequently the catalyst should be regenerated/replaced; PCO was no different. This project has focussed on time dependent depletion of degradation constants of benzene, toluene ethyl benzene, p-m xylene, o-xylene and suggested the ways to adopt the VOC degradation constant. The complete oxidation of VOCs does not happen instantly. Some intermediates are formed due to partial oxidation and can get released in the surrounding air which may be harmful to the building occupants. In addition to vapour phase intermediates, some partially oxidised semi-volatiles can deposit on the catalyst surface and may be released when catalyst is regenerated. This study assessed exposure risk of intermediates and has suggested the pathways of degradation of BTEX.

The major focus of the study was to pilot test the technology in the field-worthy and addresses all the issues of technology up-gradation. Specifically new equipment was designed based on the degradation rates estimated from laboratory studies (carried out in this project) reduction in the efficacy of catalyst with its use. The impediment and difficulties encountered in earlier versions have been taken in consideration while designing the new units which is easy to operate and cost effective as pressure drop has been reduced significantly. The technology is at a stage where it can be adopted by the industry.

6.2 Conclusions

Based on the analyses of results, the following conclusions are drawn:

A standardized TiO₂ sol gel coating method is established based on characterization of catalyst surface for structural continuity, surface roughness, surface impurities, strong surface attachment and particle size. The particle size of coated TiO₂ was in nano size (10.2±1.43 nm) that should ensure large active surface area (around 100 m²/g) of catalyst.

This study has estimated the degradation rate for UV lamps of 8W, 11W and 16W. The highest degradation rate (for all VOCs) was obtained for 16W lamp. The higher wattage of lamp results in increased running cost but there is an opportunity to optimize the process based on increased wattage versus increased efficiency of the PCO system.

For a stable performance of the reactor, the challenge was to accommodate continuous deactivation of the catalyst surface which adversely affected the degradation rate, k. An incorrect value of k (which is decreasing with time of operation) results in inadequate design of process

and its poor performance. For a thirteen hour operation and regeneration cycle, the average k value (for BTEX) ranges from $0.80 \text{ min}^{-1} \text{ m}^{-2}$ to $0.95 \text{ min}^{-1} \text{ m}^{-2}$ for 8W UV and $1.00 \text{ min}^{-1} \text{ m}^{-2}$ to $1.66 \text{ min}^{-1} \text{ m}^{-2}$ for 16W UV lamps. It is proposed that for 8W UV lamps the k value should be taken as $0.87 \text{ min}^{-1} \text{ m}^{-2}$ (average of the range of k value) and for 16W UV lamps, it should be $1.3 \text{ min}^{-1} \text{ m}^{-2}$.

Three methods (heating at $450 \text{ }^\circ\text{C}$, washing with H_2O_2 and irradiation by UV lamp) of catalyst regeneration were examined. Although these methods can regenerate the catalyst in the range 92-98 percent of original k value, it is concluded that the heating of reactor is the fastest and most efficient regeneration technique and should be followed.

In the long-term laboratory experiments over two years, reactors have been regenerated over several times (by heating at 450°C) and their performance has been acceptable in terms of degradation rates. It is concluded that the regenerated catalyst can be used for a reasonable time; however, one should examine the catalyst performance for degradation of VOCs and its mechanical strength for long-term uses.

This study has taken the technology to field and demonstrated its effectiveness for different VOCs (benzene, Mono, Di, and Tri chlorobenzene, and mixture of solvents present in chemistry laboratory). The estimated degradation rate constant for coexisting multiple VOCs was $1.06 \text{ min}^{-1} \text{ m}^{-2}$ (surface area of catalyst), which in comparison to that of benzene ($1.6 \text{ min}^{-1} \text{ m}^{-2}$), is smaller by 34% because of concurrent competitive reactions on the surface of catalyst. The control efficiency of device was over 99 percent for benzene, 88 percent for multiple VOCs and 71 percent for chlorobenzenes.

The intermediates of degradation of BTEX (both in vapour phase (except benzene) and those from catalyst regeneration) were quantified and human health risk of exposure of these intermediates was assessed. The carcinogenic risk and Hazard Index (HI) both were within acceptable level and technology can be adopted in field without any fear of unacceptable risk from the intermediates.

The new equipment, designed based on the degradation rates estimated from laboratory studies (carried out in this project) of reduction in the efficacy of catalyst with its use has also been tested. The impediment and difficulties encountered in earlier versions have been taken in consideration while designing the new units which is easy to operate and cost effective. The technology is worthy of field application.

References

- Ameen MM, Raupp GB (1999) Reversible Catalyst Deactivation in the Photocatalytic Oxidation of Dilute o-Xylene in Air. *J Catal* 122:112–122.
- Al Momani F (2007) Treatment of air containing volatile organic carbon: Elimination and post treatment. *Environ Eng Sci* 24:1038–1047.
- Alberici RM, Jardim WF (1997) Photocatalytic destruction of VOCS in the gas-phase using titanium dioxide. *Appl Catal B Environ* 14:55–68.
- Ao CH, Lee SC, Mak CL, Chan LY (2003) Photodegradation of volatile organic compounds (VOCs) and NO for indoor air purification using TiO₂: promotion versus inhibition effect of NO. *Appl Catal B Environ* 42:119–129.
- Asante-Duah DK(1998) Risk assessment in environmental management. John Wiley and Sons, New York, NY (US), United States.
- Benoit-marquié F, Wilkenhöner U, Simon V, Braun A, OliverosE, Maurette M (2000) VOC photodegradation at the gas – solid interface of a TiO₂ photocatalyst Part I: 1-butanol and 1-butylamine. *J Photochem Photobiol A Chem* 132:225–232.
- Blount MC, Falconer JL (2002) Steady-state surface species during toluene photocatalysis. *Appl Catal B Environ* 39:39–50.
- Blount MC, Falconer JL (2001) Characterization of Adsorbed Species on TiO₂ after Photocatalytic Oxidation of Toluene. *J Catal* 33:21–33.
- Boulamanti AK, Korologos CA, Philippopoulos CJ (2008) The rate of photocatalytic oxidation of aromatic volatile organic compounds in the gas-phase. *Atmos Environ* 42:7844–7850.
- Brickus LSR, Cardoso JN, De Aquino Neto FR (1998) Distributions of Indoor and Outdoor Air Pollutants in Rio de Janeiro , Brazil : Implications to Indoor Air Quality in Bayside Offices. *Environ Sci Technol* 32:3485–3490.
- Burstyn I, Isabelle X, Cherry N, Senthilselvan A (2007) Determinants of airborne benzene concentrations in rural areas of western Canada. *Atmos Environ* 41:7778–7787.

- Byrne JA, Eggins BR, Brown NMD, MckinneyB, Rouse M (1998) Immobilisation of TiO₂ powder for the treatment of polluted water. *Appl Catal B Environ* 17:25–36.
- Cao L, Gao Zi, Suib Steven L, N OT, O HS, DFJ(2000) Photocatalytic Oxidation of Toluene on Nanoscale TiO₂ Catalysts: Studies of Deactivation and Regeneration. *J Catal* 196:253–261.
- Carp O, Huisman CL, Reller A (2004) Photoinduced reactivity of titanium dioxide. *Prog solid Sate Chem* 32:33–177.
- Černigoj U, Štangar UL, Trebše P (2007) Evaluation of a novel Carberry type photoreactor for the degradation of organic pollutants in water. *J Photochem Photobiol A Chem* 188:169–176.
- Chau JLH, Tung C, Lin Y, Li A (2008) Preparation and optical properties of titania / epoxy nanocomposite coatings. *Mater Lett* 62:3416–3418.
- Chen J, Li G, He Z, An T (2011) Adsorption and degradation of model volatile organic compounds by a combined titania – montmorillonite – silica photocatalyst. *J Hazard Mater* 190:416–423.
- Choi N., Choi J., Kim S, Park S, Kim D (2009) Two-dimensional modelling of benzene transport and biodegradation in a laboratory-scale aquifer. *Environ Technol* 30:53–62.
- Collins AM (2012) *Nanotechnology Cookbook*. Elsevier, UK.
- D’Hennezel O, Pichat P, Ollis DF (1998) Benzene and toluene gas-phase photocatalytic degradation over H₂O and HCL pretreated TiO₂: by-products and mechanisms. *J Photochem Photobiol A Chem* 118:197–204.
- Deng X, Yue Y, Gao Z (2002) Gas-phase photo-oxidation of organic compounds over nanosized TiO₂ photocatalysts by various preparations. *Appl Catal B Environ* 39:135–147.
- Deshusses M a., Webster TS (2000) Construction and economics of a pilot/full-scale biological trickling filter reactor for the removal of volatile organic compounds from polluted air. *J Air Waste Manage Assoc* 50:1947–1956.
- Dhada I (2008) TiO₂ based photocatalytic oxidation of benzene, toluene and p- xylene. Master of Technology, Indian Institute of Technology Kanpur.

- Dhada I, Nagar PK, Sharma M (2015a) Photo-catalytic oxidation of individual and mixture of benzene, toluene and p-xylene. *Int J Environ Sci Technol*. doi: 10.1007/s13762-015-0783-4.
- Dhada I, Nagar PK, Sharma M (2015b) Challenges of TiO₂ -based photooxidation of volatile organic compounds: designing, coating, and regenerating catalyst. *Ind Eng Chem Res* 54:5381–5387.
- Dhada I, Sharma M, Gupta T, Agarwal S, Mohanan R (2012) TiO₂-based photo catalytic oxidation of VOCs: coating to reactor performance and design. International Conference on Environmental Science and Technology, American Academy of Sciences, Houston, USA.
- Dutta C, Som D, Chatterjee A (2009) Mixing ratios of carbonyls and BTEX in ambient air of Kolkata , India and their associated health risk. *Env Monit Assess* 97–107.
- Dzik P, Vesel M, Chomoucká J (2010) Thin layers of photocatalytic TiO₂ prepared by inkjet printing of a solgel precursor. *J Adv Oxid Technol* 13:172–183.
- Edgerton SA, Holdren MW, Smith DL, Shah JJ (1989) Inter-Urban Comparison of Ambient Volatile Organic Compound Concentrations in U.S. Cities. *JAPCA* 39:729–732.
- Everaert K, Baeyens J (2004) Catalytic combustion of volatile organic compounds. *J Hazard Mater* 109:113–139.
- Farhanian D, Haghghat F (2014) Photocatalytic oxidation air cleaner: Identification and quantification of by-products. *Build Environ* 72:34–43.
- Fernhdez A, Lassaletta G, Jimknez VM, Justo A (1995) Preparation and characterization of TiO₂ photocatalysts supported on various rigid supports (glass , quartz and stainless steel). Comparative studies of photocatalytic activity in water purification. *Appl Catal B Environ* 7:49–63.
- Fox MA, Dulay MT (1993) Heterogeneous Photocatalysis. *Chem Rev* 93:341–357.
- Fujishima A, Zhang X (2006) Titanium dioxide photocatalysis : present situation and future approaches. *CRChimie* 9:750–760.
- GSI Environmental (2013) GSI Chemical properties database. <http://old.gsi-net.com/en/publications/gsi-chemical-database.html>. Accessed 24 Oct 2015.

- Guo T, Bai Z, Wu C, Zhu T (2008) Influence of relative humidity on the photocatalytic oxidation (PCO) of toluene by TiO₂ loaded on activated carbon fibers: PCO rate and intermediates accumulation. *Appl Catal B Environ* 79:171–178.
- Gupta VK, Verma N (2002) Removal of volatile organic compounds by cryogenic condensation followed by adsorption. *Chem Eng Sci* 57:2679–2696.
- Hager S, Bauer R (1999) Heterogeneous photocatalytic oxidation of organic for air purification by near UV irradiated titanium dioxide. *Chemosphere* 38:1549–1559.
- Han S, Lee J, Kim JS, Oh S, Park Y, Kim H (2008) Gaseous by-products from the TiO₂ Photocatalytic Oxidation of Benzene. *Environ Eng Res* 13:14–18.
- Han X, Naeher LP (2006) Review article A review of traffic-related air pollution exposure assessment studies in the developing world. *Environ Int* 32:106–120.
- He F, Li J, Li T, Li G (2014) Solvothermal synthesis of mesoporous TiO₂: The effect of morphology, size and calcination progress on photocatalytic activity in the degradation of gaseous benzene. *Chem Eng J* 237:312–321.
- Hoffmann MR, Martin ST, Choi W, Bahnemann DW (1995) Environmental Applications of Semiconductor Photocatalysis. *Chem Rev* 95: 69–96.
- Hong I (2006) VOCs Degradation Performance of TiO₂ Aerogel Photocatalyst Prepared in SCF Drying. *J Ind Eng Chem* 12:918–925.
- Jacoby WA, Blake DM, Fennell JA, Boulter J E, Vargo L M, George M C, Dolberg S K (1996) Heterogeneous photocatalysis for control of volatile organic compounds in indoor air. *J Air Waste Manage Assoc* 46:891–898.
- Jagannathan K, Swaminathan T (2011) Removal of gas-phase benzene in an immobilized photocatalytic reactor. The dramatic and debilitating effects of air pollution are a matter of increasing regulatory concern. The 1990 Clean Air Act Amendments, proposed by the USEPA is the most recent ver-. *Maced J Chem Eng* 30:221–228.
- Jang HD, Kim S, Kim S (2001) Effect of particle size and phase composition of titanium dioxide nanoparticles on the photocatalytic properties. *J Nanoparticle Res* 141–147.

- Jeong J, Sekiguchi K, Lee W, Sakamoto K (2005) Photodegradation of gaseous volatile organic compounds (VOCs) using TiO₂ photoirradiated by an ozone-producing UV lamp: decomposition characteristics, identification of by-products and water-soluble organic intermediates. *J Photochem Photobiol A: Chem* 169:279–287.
- Jeong J, Sekiguchi K, Sakamoto K (2004) Photochemical and photocatalytic degradation of gaseous toluene using short-wavelength UV irradiation with TiO₂ catalyst: comparison of three UV sources. *Chemosphere* 57:663–671.
- Jo W, Park K (2004) Heterogeneous photocatalysis of aromatic and chlorinated volatile organic compounds (VOCs) for non-occupational indoor air application. *Chemosphere* 57:555–565.
- K K, L O, L M, Placha D, Lacny Z, Jirkovsky J (2009) Effect of TiO₂ particle size on the photocatalytic reduction of CO₂ in olcova. *Appl Catal B Environ* 89:494–502.
- Kachina A (2008) Gas-phase photocatalytic oxidation of volatile Organic Compounds. Doctor of Science, Lappeenranta University of Technology.
- Keshmiri M, Troczynski T, Mohseni M (2006) Oxidation of gas phase trichloroethylene and toluene using composite sol – gel TiO₂ photocatalytic coatings. *J Hazard Mater* 128:130–137.
- Kim DH, Anderson MA (1994) Photoelectrocatalytic degradation of formic acid using a porous TiO₂ thin-film electrode. *Environ Sci Technol* 479–483.
- Kim SB, Hyun HT, Sung H chang (2002) Photocatalytic degradation of volatile organic compounds at the gas – solid interface of a TiO₂ photocatalyst. *Chemosphere* 48:437–444.
- Korologos CA, Nikolaki MD, Zerva CN, Philippopoulos CJ, Pouloupoulos S G (2012) Photocatalytic oxidation of benzene, toluene, ethylbenzene and m-xylene in the gas-phase over TiO₂-based catalysts. *Journal Photochem Photobiol A: Chem* 244:24–31.
- Korologos CA, Philippopoulos CJ, Pouloupoulos SG (2011) The effect of water presence on the photocatalytic oxidation of benzene, toluene, ethylbenzene and m-xylene in the gas-phase. *Atmos Environ* 45:7089–7095.

- Lau W, Chan L (2003) Commuter exposure to aromatic VOCs in public transportation modes in Hong Kong. *Sci Total Environ* 308:143–155.
- Lichtin NN (1996) TiO_2 -Photocatalyzed Oxidative Degradation of CH_3CN , CH_3OH , C_2HCl_3 , and CH_2Cl_2 Supplied as Vapours and in Aqueous Solution under Similar Conditions. *Environ Sci Technol* 30:2014–2020.
- Lü H, Wen S, Feng Y, Wang X, Bi X (2006) Indoor and outdoor carbonyl compounds and BTEX in the hospitals of Guangzhou, China. *Sci Total Environ* 368:574–584.
- Maira AJ, Yeung KL, Soria J, Coronado J M, Belver C, Lee C Y, Augugliaro V (2001) Gas-phase photo-oxidation of toluene using nanometer-size TiO_2 catalysts. *Appl Catal B Environ* 29:327–336.
- Matsunaga T, Yamaoka H, Ohtani S, Harada Y, Fujii T (2008) High photocatalytic activity of palladium-deposited mesoporous $\text{TiO}_2/\text{SiO}_2$ fibers. *Appl Catal A: General* 351:231–238.
- Mo J, Zhang Y, Xu Q, Joaquin J, Zhao R (2009a) Photocatalytic purification of volatile organic compounds in indoor air: A literature review. *Atmos Environ* 43:2229–2246.
- Mo J, Zhang Y, Xu Q, Zhu Y, Joaquin J, Zhao R (2009b) Determination and risk assessment of by-products resulting from photocatalytic oxidation of toluene. *Appl Catal B Environ* 89:570–576.
- Nagar P K (2010) TiO_2 -based Photocatalytic Control of Volatile Organic Compounds: Enhancing the Reactor Performance, Master of Technology, Indian Institute of Technology Kanpur.
- Nguyen HT, Miao L, Tanemura S, Tanemura M (2004) Structural and morphological characterization of anatase TiO_2 coating on γ -Alumina scale fiber fabricated by sol – gel dip-coating method. *J Cryst Growth* 271:245–251.
- Obee TN, Hay SO (1997) Effects of Moisture and Temperature on the Photooxidation of Ethylene on Titania. *Environ Sci Technol* 31:2034–2038.
- Ollis DF (2000) Photocatalytic purification and remediation of contaminated air and water. *Surf Chem Catal* 3:405–411.

- Peral J, Ollis DF (1997) TiO₂ , photocatalyst deactivation by gas-phase oxidation of heteroatom organics. *Journal of molecular Catalysis A:Chemical* 115:347-354
- Piera E, Ayllón JA, Doménech X, Peral J (2002) TiO₂ deactivation during gas-phase photocatalytic oxidation of ethanol. *Catal Today* 76:259–270.
- Pingxiao W, Jianwen T, Zhi D (2007) Preparation and photocatalysis of TiO₂ nanoparticles doped with nitrogen and cadmium. *Mater Chem Phys* 103:264–269.
- Puddu V, Choi H, Dionysiou DD, Puma GL (2010) TiO₂ photocatalyst for indoor air remediation: Influence of crystallinity, crystal phase, and UV radiation intensity on trichloroethylene degradation. *Appl Catal B Environ* 94:211–218.
- Rafael M-R, Cardona-martõ N (1998) Relationship between the formation of surface species and catalyst deactivation during the gas-phase photocatalytic oxidation of toluene. *Catal Today* 40:353–365.
- Rene ER, Murthy DVS, Swaminathan T (2005) Performance evaluation of a compost biofilter treating toluene vapours. *Process Biochem* 40:2771–2779.
- Sakatani Y, Grosso D, Nicole L (2006) Optimised photocatalytic activity of grid-like mesoporous TiO₂ films: effect of crystallinity , pore size distribution , and pore accessibility. *J Mater Chem* 33:1–6.
- Salaices M, Serrano B, Lasa HI De (2004) Photocatalytic conversion of phenolic compounds in slurry reactors. *Chem Eng Sci* 59:3–15.
- Sauer ML, Ollis DF (1996) Catalyst Deactivation in Gas – Solid Photocatalysis. *J Catal* 217:215–217.
- Sexton K, Adgate JL, Mongin SJ, Pratt GC, Ramachandran G, StockTH, Morandi MT (2004) Evaluating differences between measured personal exposures to volatile organic compounds and concentrations in outdoor and indoor air. *Environ Sci Technol* 38:593–602.
- Shuang-shi D, Jian-bin Z, Lin-lin GAO, Yan-long W, Dan-dan Z (2012) Preparation of spherical activated carbon-supported and Er³⁺: YAlO₃-doped TiO₂ photocatalyst for methyl orange degradation under visible light. *Trans Nonferrous Met Soc China* 22:2477–2483.

- Sleiman M, Conchon P, Ferronato C, Chovelon J-M (2009) Photocatalytic oxidation of toluene at indoor air levels (ppbv): Towards a better assessment of conversion, reaction intermediates and mineralization. *Appl Catal B Environ* 86:159–165.
- Song Y, Saho M, Liu Y, Lu S, Kuster W, Goldan P, Xie S (2007) Source Apportionment of Ambient Volatile Organic Compounds in Beijing. *Environ Sci Technol* 41:4348–4353.
- Srivastava A, Joseph A., More A, Patil S (2005) Emissions Of Vocs At Urban Petrol Retail Distribution Centres In India (Delhi And Mumbai). *Environ Monit Assess* 227–242.
- Tejasvi R, Sharma M, Upadhyay K (2015) Passive photo-catalytic destruction of air-borne VOCs in high traffic areas using TiO₂-coated flexible PVC sheet. *Chem Eng J* 262:875–881.
- USEPA (2003) Cyclohexane ; CASRN 110-82-7.
- USEPA (2006) The Clean Air Act Amendments of 1990. <http://www.epa.gov/air/caa/>. Accessed 10 Dec 2010.
- USEPA(2011) An Introduction to Indoor Air Quality (IAQ). In: Indoor Air. <http://www.epa.gov/iaq/voc.html>. Accessed 6 Jun 2015.
- Wang S, Ang HM, Tade MO (2007) Volatile organic compounds in indoor environment and photocatalytic oxidation: State of the art. *Environ Int* 33:694–705.
- Weisel CP, Alimokhtari S, Sanders PF (2008) Indoor Air VOC Concentrations in Suburban and Rural New Jersey. *Environ Sci Technol* 42:8231–8238.
- Xiao G, Huang A, Su H, Tan T (2013) The activity of acrylic-silicon / nano- TiO₂ films for the visible-light degradation of formaldehyde and NO₂. *Build Environ* 65:215–221.
- Yan T, Long J (2010) Efficient Photocatalytic Degradation of Volatile Organic Compounds by Porous Indium Hydroxide Nanocrystals. *Environ Sci Technol* 44:1380–1385.
- Yen C, Wang D, Shih M, Chang L, Shih HC(2010) Applied Surface Science A combined experimental and theoretical analysis of Fe-implanted TiO₂ modified by metal plasma ion implantation. *Appl Surf Sci* 256:6865–6870.
- Yoon KH, Noh JS, Kwon CH, Muhammed M (2006) Photocatalytic behavior of TiO₂ thin films prepared by sol-gel process. *Mater Chem Phys* 95:79–83.

- You XI, Senthilselvan A, Cherry NM, Kim H (2008) Determinants of airborne concentrations of volatile organic compounds in rural areas of Western Canada. *J Expo Sci Environ Epidemiol* 117–128.
- Yu-Zhang K, Boisjolly G, Rivory J, Kilian L, Colliex C(1994) Characterization of TiO₂/SiO₂ multilayers by high resolution transmission electron microscopy and electron energy loss spectroscopy. *Thin solid Films* 253:299–302.
- Zhang M, An T, Fu J, Sheng G (2006) Photocatalytic degradation of mixed gaseous carbonyl compounds at low level on adsorptive TiO₂ / SiO₂ photocatalyst using a fluidized bed reactor. *Chemosphere* 64:423–431.
- Zhang Y, Mu Y, Liu J, Mellouki A (2012) Levels , sources and health risks of carbonyls and BTEX in the ambient air of. *J Environ Sci* 24:124–130.
- Zhong J, Wang J, Tao L, Gong M, Zhimin L, Chen Y (2007) Photocatalytic degradation of gaseous benzene over TiO₂ / Sr₂ CeO₄: Kinetic model and degradation mechanisms. *J Hazard Mater* 139:323–331.
- Zhu J, Newhook R, Marro L, Chan CC (2005) Selected volatile organic compounds in residential air in the city of Ottawa, Canada. *Environ Sci Technol* 39:64–71.

Appendix- A

Table S1: Probable by-products of BTEX with their RT in GC-MS

Benzene intermediates	Ethylbenzene intermediates	p, m-xylene intermediates	o-xylene intermediates	Toluene intermediates
1-methyl-1-ethyl cyclobutane(17.69); 1-butyl cyclobutanol(15.49); cyclopropane(21.11); 2-methyl phenol(21.34), 4-methyl phenol-(4-cresol) (21.98), Methyl cyclopentane (9.54). 2,2,4-trimethyl hexane and 2,2,3 trimethyldecane(8.2), 2-methyl-3-butan-1-ol(7.20), m-phenethylbenzotrile and 4-(phenyl methoxy)-1,2,5-oxadiazol-3-amine(13.44)	Methyl cyclopentane (9.54); Methyl alpha, D-rhamnopyranoside(10.86); alpha-L-galactopyranoside(10.86); Propanoic acid (12.86); Benzene (phenoxymethyl)(13.42); ethanone,2hydroxy-1,2-diphenyl(21.23); 4-methylphenol(21.99) ; Cyclohexanol 4 methyl(23.56); Acetophenone 4-hydroxy (23.85); Benzoicacid-4-methyl(26.93) and Tetra Decanoic acid (27.33);	1,2,3,4 tetramethylcyclobutane (9.5); Benzene phenoxymethyl(13.42); 2-propane-1-one,1,3-diphenyl(13.127); Benzene(1-cyclohexylethyl)(15.57); 3-methyl benzoicacid(26.7) and 4-methyl benzoicacid(26.93)	Trimethyldecane (8.28); 1,2,3,4 tetrmethylcyclobutane (9.5); D-ribonicacidgammalact one(10.87); 4-methyl phenol(21.95) and N-hexadecanoic acid(27.34);	Trimethyldecane(8.32); Methylcyclopentane(9.58); 1-butanol-4-butoxy(11.04); Fumaric acid(16.25);1 butyl cyclobutanol(15.49); 2-pentacosanone (17.34);1-methyl-1-ethylcyclobutane(17.69); Cyclopropane, 1-(2-methyl butyl)-1-(-1 methylpropane)(21.11); 2-methylphenol,(21.34) P-cresylisovalerate (22.00);1,3-bis-t-Butylperoxy-phthalan(24.42); 4-acetylphenyl-5-acetyl-2- methoxy phenyl ether(24.87) and Methanone, (1 hydroxycyclohexyl)phenyl(26.07)

Numerical values in bracket is retention time in minute

Appendix-B

Table S2: Indoor air concentration of by-products (Vapour and solid phase) of PCO of p,m-xylene and long-term health risk (Volume of room 195m³ and mass of p, m xylene treated 2.106mg

Intermediates	CA (mg/m ³)	CDI (mg/kg-day)	RfD (mg/kg-day)	Carcinogenic Risk(SF*CDI)	HI
Vapour phase					
Pentane	1.44E-05	1.36E-06	@		
Toluene	2.63E-05	2.50E-06	1.40E+00		1.79E-06
1,4 benzoquinone	1.12E-05	1.06E-06	@		
Benzylalcohol	4.96E-05	4.70E-06	3.00E-01		1.57E-05
Benzoic acid	1.19E-04	1.13E-05	4.00E+00		2.83E-06
Hydroquinone	1.15E-04	1.09E-05	@		
			Σ=	0.00E+00	2.03E-05
Solid phase					
Acetone	8.21E-06	7.79E-07	1.00E-01		7.79E-06
Hexane	1.55E-04	1.47E-05	5.72E-02		2.57E-04
Cyclohexane	5.27E-08	5.00E-09	1.71E+00 [#]		2.92E-09
Benzene	2.18E-11	2.07E-12	2.90E-01*	6.00E-14	
Crotonaldehyde	5.88E-06	5.58E-07	1.90E+00*	1.06E-06	
Toulene	4.90E-10	4.64E-11	1.40E+00		3.32E-11
1,4-benzoquinone	9.51E-08	9.02E-09	@		
Benzaldehyde	1.74E-07	1.65E-08	1.00E-01		1.65E-07
Phenol	7.11E-07	6.74E-08	6.00E-01		1.12E-07
Benzyl alcohol	1.58E-07	1.50E-08	3.00E-01		5.00E-08
Cresol	1.37E-06	1.30E-07	5.00E-02		2.59E-06
Hydroquinone	2.21E-06	2.09E-07	@		
Benzoic acid	9.97E-06	9.46E-07	4.00E+00		2.36E-07
			Σ =	1.06E-06	2.68E-04
Overall risk (vapourphase+solid phase) =				1.06E-06	2.89E-04

@ RfD is not available for pentane, 1,4 benzoquinone and hydroquinone

(U.S.E.P.A(US Environmental Protection Agency) 2003)

^o (GSI Environmental 2013)

* Slope factor, slope factor for Crotonaldehyde is =1.9/mg/kg/day (GSI Environmental 2013)
carcinogenic risk (CDI×SF)

Table S3: Indoor air concentration of intermediates (Vapour and solid phase) of PCO of o-xylene and long-term health risk (Volume of room 195 m³ and mass of o-xylene treated 1.404mg)

Intermediates	CA (mg/m ³)	CDI (mg/kg-day)	RfD (mg/kg-day)	Carcinogenic Risk(SF×CDI)	HI
Vapour phase					
Acetone	1.36E-06	1.29E-07	6.67E-02		1.29E-06
Hexane	4.99E-04	4.73E-05	3.82E-02		8.27E-04
Phenol	2.35E-05	2.23E-06	4.00E-01		3.72E-06
Benzoic acid	1.22E-04	1.15E-05	2.67E+00		2.88E-06
Hydroquinone	1.02E-04	9.68E-06	@		
Σ=				0.00E+00	8.35E-04
Solid phase					
Acetone	1.33E-04	1.26E-05	6.67E-02		1.26E-04
Hexane	6.79E-05	6.44E-06	3.82E-02		1.13E-04
Cyclohexane	7.45E-08	7.07E-09	1.14E+00 [#]		4.13E-09
Benzene	4.30E-11	4.08E-12	1.90E-01*	1.18E-13	
Crotonaldehyde	2.60E-06	2.47E-07	1.27E+00*	4.69E-07	
Toulene	1.92E-10	1.83E-11	9.34E-01		1.30E-11
1,4-benzoquinone	2.29E-07	2.17E-08	@		
Benzaldehyde	2.04E-06	1.93E-07	6.67E-02		1.93E-06
Phenol	8.40E-07	7.97E-08	4.00E-01		1.33E-07
Benzyl alcohol	2.25E-07	2.14E-08	2.00E-01		7.12E-08
Cresol	5.16E-06	4.89E-07	3.34E-02		9.79E-06
Hydroquinone	1.04E-06	9.89E-08	@		
Benzoic acid	9.83E-06	9.32E-07	2.67E+00		2.33E-07
Σ =				4.69E-07	2.51E-04
Overall (vapourphase+solid phase) =				4.69E-07	1.09E-03

@ RfD is not available for 1,4 benzoquinone and hydroquinone

(U.S.E.P.A(US Environmental Protection Agency) 2003)

° (GSI Environmental 2013)

* Slope factor, slope factor for Crotonaldehyde is =1.9/mg/kg/day(GSI Environmental 2013) carcinogenic risk (CDI×SF)

Table S4: Indoor air concentration of intermediates (Vapour and solid phase) of PCO of toluene and long-term health risk (Volume of room 195 m³ and mass of toluene treated 1.73mg)

Intermediates	CA (mg/m ³)	CDI (mg/kg- day)	RfD (mg/kg- day)	carcinogenic Risk=(SF*CDI)	HI
Vapour phase					
Acetone	2.32E-05	2.2E-06	6.67E-02		2.2E-05
Hexane	2.49E-05	2.37E-06	3.82E-02		4.14E-05
Benzyldehyde			6.67E-02		
	2.20E-05	2.08E-06			2.08E-05
Benzoic acid	1.68E-04	1.59E-05	2.67E+00		3.99E-06
Hydroquinone	1.03E-04	9.74E-06	@		
			Σ =	0.00E+00	8.82E-05
Solid phase					
Acetone	2.19E-04	2.07E-05	1.00E-01		2.07E-04
Hexane	7.61E-06	7.22E-07	5.72E-02		1.26E-05
Cyclohexane	3.34E-08	3.17E-09	1.71E+00 [#]		1.85E-09
crotonaldehyde	8.75E-09	8.30E-10	1.90E+00* @	1.58E-09	
1,4- benzoquinone	3.27E-06	3.1E-07			
Benzaldehyde	2.36E-07	2.24E-08	0.1		2.24E-07
Phenol	1.87E-06	1.77E-07	6.00E-01		2.95E-07
Benzyl alcohol	2.35E-06	2.23E-07	3.00E-01		7.42E-07
Cresol	2.26E-06	2.14E-07	5.00E-02		4.29E-06
Hydroquinone	1.15E-05	1.09E-06	@		
Benzoic acid	1.57E-05	1.49E-06	4.00E+00		3.73E-07
			Σ =	1.58E-09	2.26E-04
			Overall (Vapourphase+solid phase) =	1.58E-09	3.14E-04

@ RfD is not available for 1,4 benzoquinone and hydroquinone

(U.S.E.P.A(US Environmental Protection Agency) 2003)

o (GSI Environmental 2013)

* Slope factor, slope factor for crotonaldehyde is =1.9/mg/kg/day (GSI Environmental 2013) carcinogenic risk (CDI×SF)

